Spectral stability of travelling waves in the Fisher-Kolmogorov-Petrovsky-Piskunov and Fisher-Stefan models

Thi Thu Huong Bui

A thesis submitted in partial fulfillment of
the requirements for the degree of
Master of Philosophy

Applied Mathematics
University of Sydney

June 2023

Certificate of Authorship/Originality

I certify that to the best of my knowledge, the content of this thesis is my own work. This thesis has not been submitted for any degree or other purposes.

I also certify that the intellectual content of this thesis is the product of my own work and that all the assistance received in preparing this thesis and sources have been acknowledged.

Thi Thu Huong Bui

ABSTRACT

Spectral stability of travelling waves in the Fisher-Kolmogorov-Petrovsky-Piskunov and Fisher-Stefan models

by
Thi Thu Huong Bui

The reaction-diffusion equations including the Fisher-Kolmogorov-Petrovsky-Piskunov (Fisher-KPP) and Fisher-Stefan model have been used to study biological invasion. Such travelling wave solutions have successfully illustrated invasive phenomena in the ecosystem. In this thesis, we first consider the standing waves and travelling waves of the Fisher-KPP equation and the behaviour of the dynamical system near the equilibrium points.

Next, we examine the existence of solutions to the Fisher-KPP model by constructing a trapping region in the plane for the wave speed $c \neq 0$. Then, we study stability of standing waves and travelling waves of this model by looking at the point spectrum, the asymptotic operator and the essential spectrum. We notice that the spectrum in the right half of plane implies that the travelling waves are unstable when $c > 0$. However, a limitation of the Fisher-KPP equation is that it cannot be used to model the extinction of invasive populations in practical situations. Hence, the Fisher-Stefan equation is introduced to simulate both biological invasion for $c > 0$ and recession for $c < 0$. This model is reformulated from the Fisher-KPP equation and includes a moving boundary, which gives rise to a spreading-vanishing dichotomy.

Moreover, we look at the existence and uniqueness of solutions to the Fisher-Stefan equation. By analysing the phase portrait, numerical results and the perturbation solutions, we can construct approximate solutions of the Fisher-Stefan equation. This phase portrait of this model also suggests that the solutions of the Fisher-KPP model exist for $c < 2$ but they are unstable. Therefore, these solutions are disregarded when $c < 2$ and considered as not exist. This unstable solution has value in describing solution of Fisher-Stefan problem. Thus, the stable solutions exist in the Fisher-Stefan problem.

Last, we consider the spectral stability of the Fisher-Stefan equation by analysing its asymptotic operator, continuous spectrum and point spectrum. The results indicate that there is no point spectrum of the Fisher-Stefan asymptotic solution for the eigenvalue parameter $\lambda > 1$ at $c \geq 0$.

Acknowledgements

First and foremost, I would like to express my sincere gratitude and appreciation to my supervisor Assoc. Prof. Robert Marangell for his tremendous support, patience and encouragement during my research. His intellectual guidance, constructive feedback and valuable advice motivated me to improve my thesis and challenge myself. Through our meetings and discussions, his immense knowledge broadened my horizon and helped me to discover many new aspects of my topic. The profound knowledge I obtained from my supervisor is a precious gift that I will never forget.

Last but surely not least, I would like to thank my mother, Ms. Minh Nguyet Nguyen. Her dedication, hard work and continuous support have inspired me to never give up when facing struggles in learning and in life. I am deeply thankful for her sacrifice and unconditional love to shape my thinking and who I am today.

CONTENTS

CHAPTER 1

Introduction

The Fisher-Kolmogorov-Petrovsky-Piskunov (Fisher-KPP) equation has been used to model the invasion of species in populations and the spatial spreading of invasive species in ecology [**Fis37**]. Initially, this model was to study population genetics where u indicates the density of an advantageous gene and the travelling wave solution denotes the spread of the gene. Canosa studied a non-linear eigenvalue problem to obtain the travelling waves of Fisher's non-linear diffusion equation and describe the propagation of the mutant in a habitat [**Can73**]. The phase plane analysis of the wave profiles in [**Can73**] demonstrated that the propagation speed of the waves was linearly proportional to their thickness. Aronson and Weinberger also investigated the behaviour of solutions of the semi-linear diffusion equation for large values of the time t [**AW75**]. They let the population be distributed in a one-dimensional habitat and applied the Fisher formula. Their research considered the gene at a specific locus in a particular chromosome pair occurring in two forms called alleles. The population was then divided into three classes or genotypes including homozygotes aa or AA and heterozygotes aA. They looked at the linear densities of the genotypes at time t and incorporated the Fisher model to analyse the birth and death rates. In another study by Sherratt, he discussed the linearisation of the Fisher-KPP model about $u = 0$ and solved this equation using Laplace transforms [**She98**]. The approach of Laplace transforms to solve a piecewise linear version of the Fisher-KPP equation was also used by Sleeman and Tuma earlier [**ST84**]. However, Sherratt concentrated on large time behaviour and linearising about $u = 0$ [**She98**]. Another application of Fisher's model of dispersal in ecology and evolutionary biology was researched by Levin, Muller-Landau, Nathan and Chave [**LMLNC03**]. Their study looked at the spread of advantageous alleles in a new linear habitat and assumed that population growth was logistic [**LMLNC03**]. In another ecological context, Skellam considered the rates of advance of invading species and the distribution in space of the density of a population by random dispersal [**Ske51**]. His work embedded Fisher's problem in a broader framework and looked at dispersal kernels in multiple spatial dimensions [**Ske51**]. The idea of biological invasion particularly the stratified dispersal process was further investigated by Shigesada, Kawasaki and Takeda [**SKT95**]. Since the population expanded, new colonies were created, which caused an accelerating range expansion, they applied the Fisher model, a von Foerster equation and Skellam's model to construct a stratified diffusion model to describe the dynamics of the size distribution of colonies and estimate the range expansion in terms of rate expansion [**SKT95**].

The focus of this thesis is on investigating the existence and stability of the travelling waves and standing waves of the Fisher-KPP and Fisher-Stefan equations. The phase portrait analysis, numerical results and perturbation solutions of these models provide insights into the asymptotic operator, the essential spectrum and the continuous spectrum of the standing waves and the travelling waves.

In one space dimension, the Fisher-KPP equation is written as:

$$u_t = Du_{xx} + ru\left(1 - \frac{u}{k}\right) \quad \text{for } x \in (-\infty, \infty) \text{ and } t > 0, \tag{1.0.1}$$

where $D > 0$ is the diffusion coefficient, $r > 0$ indicates the population growth rate and $k > 0$ is the population carrying capacity.

According to Fisher, equation (1.0.1) models the change in population density when the population disperses through linear diffusion [**Fis37**]. The nonlinear reaction diffusion equation (1.0.1) is described by Fisher [**Fis37**] as:

$$u_t = ku(1-u) + Du_{xx}. \tag{1.0.2}$$

By denoting

$$t^* = kt, \tag{1.0.3}$$

and

$$x^* = x\sqrt{\frac{k}{D}}, \tag{1.0.4}$$

the logistic growth equation (1.0.2) can be non-dimensionalised as

$$u_t = u_{xx} + u(1-u). \tag{1.0.5}$$

We would like to examine the existence of solutions of the travelling waves and standing waves of equation (1.0.5) by considering $u = u(x)$. In Chapter 2 Section 2.1, we look at the plots of solutions $u(x,t)$ with initial profile $H(-x)$ on $[-50, 50]$ versus x for different wave speed c where $H(x)$ is usually defined as:

$$H(x) = \begin{cases} 0 \text{ when } x < 0, \\ \\ 1 \text{ when } x > 0. \end{cases} \tag{1.0.6}$$

Next, we transform to a moving frame $z := x - ct$ and look at solutions of the form $u(x,t) = u(z)$ for $c \neq 0$. Our aim is to establish that there exists a bounded solution to the travelling waves for $c \geq 0$, which decays to 1 as $z \to -\infty$ and when $c < 0$, this is not possible. To prove the existence of solutions, we construct a trapping region in the plane for the orbit. By analysing the phase portrait of the Fisher-KPP equation when $c \geq 0$, we observe that the travelling wave solutions between the two equilibrium points $(u(z), v(z)) = (0,0)$ and $(1,0)$ correspond to a heteroclinic trajectory. In this case, $u(z)$ and $v(z)$ are defined as:

$$\frac{du}{dz} = v,$$

and

$$\frac{dv}{dz} = -cv - u(1-u).$$

The homoclinic orbit at $c = 0$ is the boundary of the trapping region. The heteroclinic trajectory from $(1, 0)$ enters the trapping region, never leaves this region and ends at $(0, 0)$. Hence, there is a travelling wave solution decaying to $u = 1$ as $z \to -\infty$.

In Section 2.2 of Chapter 2, we study the stability of standing waves in the Fisher-KPP equation as a dynamical system on an infinite dimensional space. We let

$$\mathcal{F}(u) = u_{xx} + u(1 - u)$$

and consider the standing wave solution $h(x)$ of the Fisher-KPP model by solving

$$h_{xx} + h(1 - h) = 0. \tag{1.0.7}$$

Ideally, we would look for the Jacobian of the fixed points of $\mathcal{F}$ and its eigenvalues. However, since we do not have a Jacobian for $\mathcal{F}$, we consider the linear part of $\mathcal{F}$, L and find the operator which acts on the direction of perturbation. If $L - \lambda I$ is not an invertible operator, where $\lambda \in \mathbb{C}$, then $\lambda \in \sigma(L)$ the spectrum of L. We will analyse the essential spectrum and the point spectrum by finding $\lambda \in \mathbb{C}$ so that $L - \lambda I$ is not invertible. The essential spectrum of L is found to be the set $(-\infty, -1]$. We next look at solutions of

$$p_{xx} + (1 - 2h(x))p = \lambda p, \tag{1.0.8}$$

where λ is the eigenvalue parameter with $\lambda > -1$ so that there exists a decaying solution as $x \to \pm\infty$, and h is a solution to equation (1.0.7). Our results show that $h(x)$ is not stable and the spectrum of the linear operator L is the set

$$\sigma(L) := (-\infty, -1] \cup \left\{\frac{-3}{4}\right\} \cup \{0\} \cup \left\{\frac{5}{4}\right\}. \tag{1.0.9}$$

In Section 2.3 of Chapter 2, we analyse the stability of travelling waves in the Fisher-KPP equation. Since the travelling wave solutions $v_c(z)$ act as steady states of the partial differential equation (PDE), we linearise about $v_c(z)$. We look for $\lambda \in \mathbb{C}$ such that $L(v_c(z)) - \lambda$ is not invertible. Our aim as before is to find a Green's function in $L^2(\mathbb{R})$. Hence, we examine the constant coefficient (asymptotic) operator. The essential spectrum and the point spectrum then shed the light on the stability of the travelling waves in the Fisher-KPP equation. We found that for all $c \in \mathbb{R}$, the essential spectrum of $L(v_c(z))$ is the set bounded by two parabolas

$$\lambda_{\pm} = -k^2 \pm 1 + ick \tag{1.0.10}$$

that open leftwards in the complex plane with vertices at ± 1, where k is the imaginary part of the eigenvalue $A_{\pm}(\lambda)$. In this case, $A_{\pm}(\lambda)$ are matrices of the equation in the far-field solutions and defined as:

$$\begin{pmatrix} p \\ q \end{pmatrix}_z = \begin{pmatrix} 0 & 1 \\ \lambda + 1 & -c \end{pmatrix} \begin{pmatrix} p \\ q \end{pmatrix} =: A_-(\lambda) \begin{pmatrix} p \\ q \end{pmatrix} \text{ as } z \to -\infty, \tag{1.0.11}$$

and

$$\begin{pmatrix} p \\ q \end{pmatrix}_z = \begin{pmatrix} 0 & 1 \\ \lambda - 1 & -c \end{pmatrix} \begin{pmatrix} p \\ q \end{pmatrix} =: A_+(\lambda) \begin{pmatrix} p \\ q \end{pmatrix} \text{ as } z \to +\infty. \tag{1.0.12}$$

The spectrum between these two curves is the essential spectrum and the curves themselves are the continuous spectrum. For λ to the right of both curves, the signature of $A_{\pm}(\lambda)$ is $(-1, 1)$ and for λ to the left of both curves, the signature of $A_{\pm}(\lambda)$ is $(-1, -1)$. For λ between these two parabolas, $A_{+}(\lambda)$ has two decaying solutions as $z \to -\infty$. Next, we examine the point spectrum of the wave $v_c(z)$ for all real c values. We suppose there exists an eigenvalue λ to $L(v_c)$ for λ to the right of the two parabolas and look for a decaying solution p satisfying $Lp = \lambda p$ for $p \in L^2(\mathbb{R})$. We conclude that there is no point spectrum of $L(v_c)$ to the right of the parabolas when $c \geq 2$.

In Chapter 3, we study the Fisher-Stefan model of the form

$$u_t = u(1-u) + u_{xx} \quad \text{for } 0 < x < s(t) \text{ and } t > 0, \tag{1.0.13}$$

$$s_t = -\kappa u_x(s(t), t) \text{ at } x = s(t), \tag{1.0.14}$$

and

$$u(s(t), t) = 0 \text{ at } t > 0, \tag{1.0.15}$$

where $x = s(t)$ is the moving boundary and the parameter κ relating the speed of the travelling wave c to the shape of the density front.

The Fisher-Stefan model adapts the Fisher-KPP equation with a moving boundary. This condition overcomes the limit of the Fisher-KPP model and replicates population extinction. Du and Lin investigated the diffusive logistic model with a free boundary in one space dimension to describe the spreading of a new or invasive species [**DL10**]. They introduced an idea of the spreading-vanishing dichotomy and proposed a different approach to the understanding of the spreading of species with population density $u(t, x)$ over a one dimensional habitat. Their paper was an attempt to use the Stefan condition to study the spreading of populations. They assumed that the species only invaded further into the environment from the right end of the initial region and the spreading front expanded at a speed that was proportional to the population gradient at the front. Their research showed that a spreading-vanishing dichotomy held for equation (1.0.13) which implied as $t \to \infty$, the population either successfully established itself in the new environment (spreading) i.e. $s(t) \to \infty$ and $u(t, x) \to 1$ or the population vanished eventually (vanishing) i.e. $s(t) \to s_\infty \leq \frac{\pi}{2}$ and $u(t, x) \to 0$ in our case. Furthermore, they proved that for large time and when the spreading occurred, the expanding front moved at a constant speed. In this paper, since the Fisher-KPP equation does not allow the solution to go extinct, we look at the Fisher-Stefan equation to overcome this limitation. By letting $\tilde{z} = ct - x$ and plotting the phase portrait of the Fisher-Stefan equation on Mathematica, we show that for $0 \leq c < 2$, there exists a unique positive solution $u(z) = u_c(z)$ defined $\forall z > 0$ to the following equation

$$\begin{cases} u'' - cu' + u(1-u) = 0, \\ u(0) = 0. \end{cases}$$

From a dynamical systems point of view, this solution u_c is the stable manifold of the fixed point $(1,0)$ and $v = u'(z)$ and $u'(z) > 0$. Moreover, we analyse the phase portrait of travelling wave solutions of the Fisher-Stefan equation to further understand the existence of solutions. By letting $z = x - ct$ at $c > 0$, we find solutions of the form $u(x,t) = u(z)$. We investigate the numerical trajectory of the limiting solutions to the Fisher-Stefan equation to compare it with the Fisher-KPP equation when $0 < c < 2$ and $-2 < c < 0$. Our observation is that both models have the same phase plane (u, v) with a different boundary condition. We also consider the phase portrait of the Fisher-Stefan equation when $-2 < c < 0$ and the density profile of travelling wave solutions of the Fisher-KPP equation to compare the existence and stability of solutions. Our findings indicate that at $c < 2$, the solutions of the Fisher-KPP equation exist but are unstable. However, in the Fisher-Stefan equation, there are stable solutions describing the problem [**EHMJ+19**].

In Chapter 4, we focus on the spectral stability of the travelling waves to the Fisher-Stefan model. Following the research by El-Hachem and her colleagues [**EHMJ+19**] and by looking at numerical solutions of this equation for negative c values, we can understand the qualitative behaviour of the trajectories. Moreover, for small $c < 2$, we find perturbation approximations to describe the shape of the travelling wave solutions of the Fisher-Stefan equation. We investigate the numerical trajectories of the Fisher-Stefan model between the two equilibrium points $(1,0)$ and $(0,0)$ in the phase plane for various wave speeds c. By comparing the accuracy of $\mathcal{O}(1)$ and $\mathcal{O}(c)$ perturbation solutions, we can identify which curve provides a more accurate match to the shape of the numerical solutions [**EHMJ+19**]. Our numerical trajectories show that the $\mathcal{O}(1)$ perturbation solution provide a more accurate match to the shape of the numerical solutions when $c = -0.05$. However, this is not the case as c becomes larger. Thus, for $0 \leq c \leq 0.5$, the $\mathcal{O}(c)$ perturbation solution is considered as being more desirable in terms of providing a more accurate approximation to the shape of the numerical solutions to the Fisher-Stefan equation [**EHMJ+19**]. In addition, we look at the spectral stability of the asymptotic solution to the Fisher-Stefan equation. Denoting such a solution by $j(z,t)$, we would like to invert $\mathcal{L}(j_c(z)) - \lambda$ on $\mathbb{R}^+$. As in Chapter 2, we need to find a Green's function in $L^2(\mathbb{R}^+)$ by having decaying solutions in the far-field. We first examine the asymptotic operator and continuous spectrum of the Fisher-Stefan model and then look for the spectrum of $\mathcal{L}_\infty$ by finding decaying solutions qualitatively depending on λ. In this case, however we have only one dispersion relation coming from $-\infty$,

$$\lambda_- = -k^2 - 1 + ick. \tag{1.0.16}$$

This equation describes the continuous spectrum of the asymptotic waves to the Fisher-Stefan equation, which is a parametrised curve opening leftwards for $\lambda \in \mathbb{C}$. Next, we analyse the point spectrum of the wave $j_c(z)$. We need to find a λ to the right of the continuous spectrum satisfying

$$\mathcal{L}(j_c)p = \lambda p, \tag{1.0.17}$$

$$p(0) = 0, \tag{1.0.18}$$

and

$$\lim_{x\to-\infty} p(x) = 0. \tag{1.0.19}$$

In a similar approach as in Chapter 2 of the Fisher-KPP model, we find that there is no point spectrum of $\mathcal{L}(j_c)$ for $\lambda > 1$ of the Fisher-Stefan model for all $c > 0$.

In Chapter 5, we summarise the similarities and differences between the Fisher-KPP equation and the Fisher-Stefan equation in terms of comparing their phase planes, the stability of the travelling waves and standing waves, the asymptotic operator and the continuous spectrum. Based on these findings, we conclude the existence of solutions for each model and then further discuss about the numerical solutions of the Fisher-Stefan equation. We also consider the possibility of the future work such as the Fisher-KPP and the Fisher-Stefan model with the Allee effect or strong Allee effect.

CHAPTER 2

Existence and stability of waves in the Fisher-KPP equation

2.1. Existence of solutions - standing and travelling waves in the Fisher-KPP equation

In this chapter, we analyse the standing and travelling waves in the Fisher-KPP equation. Using Mathematica, we plot the solutions $u(x,t)$ to equation (1.0.5) with initial profile $H(-x)$ on $[-50,50]$ versus x for $t = 0, 1, 5, 10$ and 20 as shown in Figure 1. In this case, $H(x) = 0$ for $x < 0$ and $H(x) = 1$ for $x > 0$. We let $u = u(t)$, then equation (1.0.5) becomes the logistic equation

$$u_t = u(1-u). \tag{2.1.1}$$

If we let $f(u) = u(1-u)$, equation (2.1.1) has two fixed points at $u = 0$ and $u = 1$. This implies that u increases in time since $f'(u) > 0$, and u decreases in time since $f'(u) < 0$. Therefore, the fixed point $u = 0$ is unstable in time while the fixed point $u = 1$ is stable in time.

Now we consider $u = u(x)$, then equation (1.0.5) becomes

$$u(1-u) + u_{xx} = 0. \tag{2.1.2}$$

In the phase portrait we have

$$u_x = v,$$

and

$$v_x = -u(1-u).$$

Hence,

$$\frac{\frac{dv}{dx}}{\frac{du}{dx}} = \frac{-u(1-u)}{v} = \frac{dv}{du} \tag{2.1.3}$$

$$\implies v\,dv = -u(1-u)\,du$$

$$\implies \frac{v^2}{2} = \frac{u^3}{3} - \frac{u^2}{2} + C \quad \text{where } C \text{ is a constant.}$$

Therefore, the phase plane curves need to satisfy

$$K(u,v) = \frac{v^2}{2} - \frac{u^3}{3} + \frac{u^2}{2} = C. \tag{2.1.4}$$

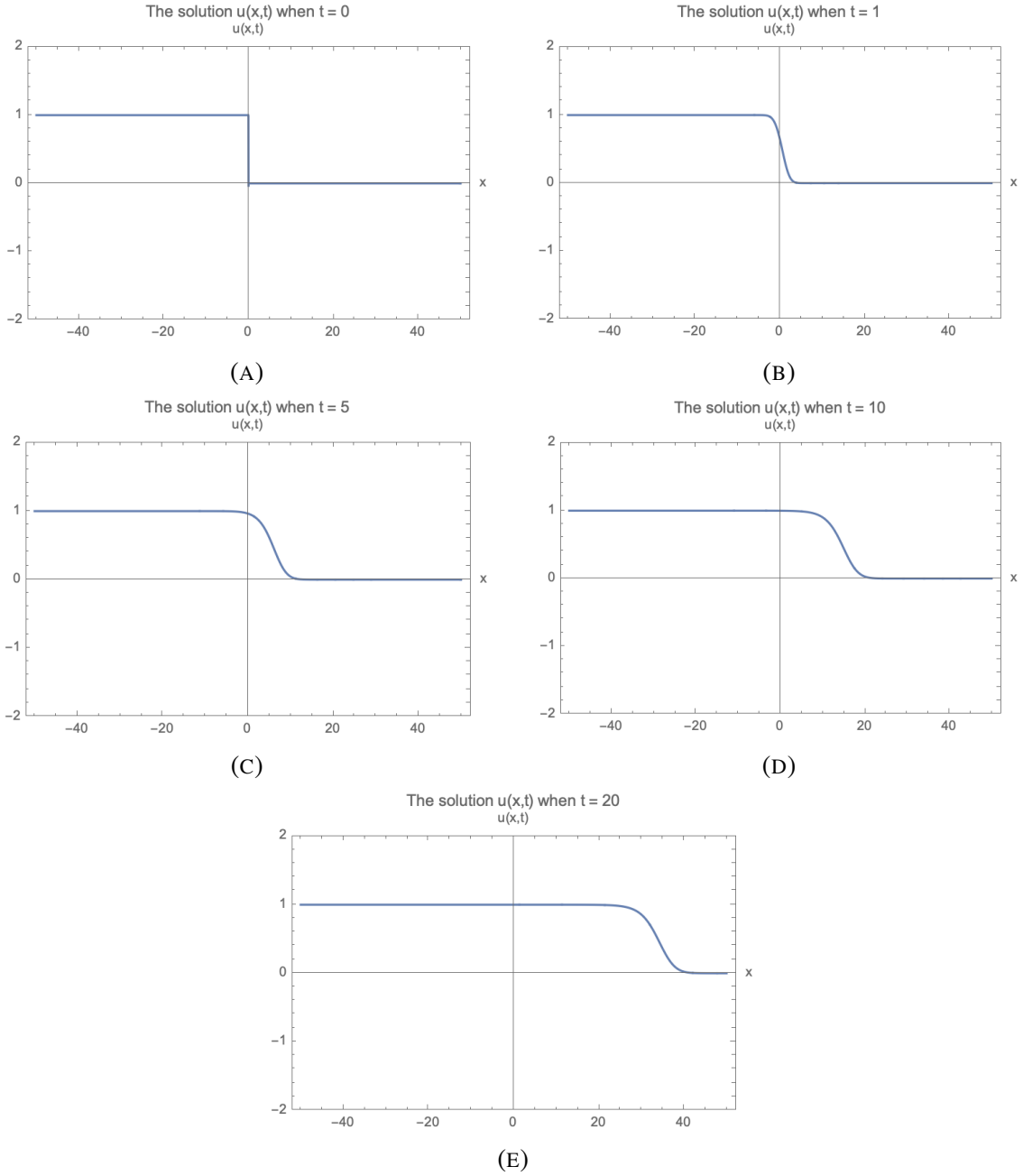

FIGURE 1. The plots of the solution $u(x,t)$ to equation (1.0.5) with initial profile equal to $H(-x)$ on [-50,50] versus x for various values of $t \geq 0$. $H(x)$ is the usual Heaviside function given by $H(x) = 0$ for $x < 0$ and $H(x) = 1$ for $x > 0$. The solution instantly smooths out, and becomes a travelling wave moving to the right.

The phase portrait curve can be seen in Figure 2 panel A. By transforming Fisher-KPP equation to a moving frame $z := x - ct$, we look for solutions of the form:

$$u(x,t) = u(x - ct) = u(z), \tag{2.1.5}$$

where $u(x,t)$ moves at finite and constant speed $c \neq 0$.

In the travelling wave coordinate, equation (1.0.5) reduces to a second order nonlinear ordinary differential equation:

$$\frac{d^2u}{dz^2} + c\frac{du}{dz} + u(1-u) = 0 \text{ for } z \in \mathbb{R}, \tag{2.1.6}$$

with the boundary conditions

$$u(-\infty) = 1, \ u(\infty) = 0 \text{ and } -\infty < z < \infty. \tag{2.1.7}$$

We now examine the existence of the solutions in equation (2.1.6) by finding the trapping region such that for $c \neq 0$, the trajectory runs from $(1,0)$, enters the region that it cannot leave and moves towards $(0,0)$. This argument follows the argument in [**Ada17**].

2.1.1. Phase portrait analysis of the Fisher-KPP equation.

We re-write equation (2.1.6) as a first order dynamical system

$$\frac{du}{dz} = v, \tag{2.1.8}$$

and

$$\frac{dv}{dz} = -cv - u(1-u). \tag{2.1.9}$$

Equation (2.1.8) and equation (2.1.9) have two equilibrium points at $(0,0)$ and $(1,0)$.

The heteroclinic trajectory between these two equilibrium points corresponds to travelling wave solutions. To prove the existence of a bounded solution for $c \geq 0$, which decays to 1 as $z \to -\infty$, we need to construct a trapping region in the plane for the orbit. We use Mathematica to model the phase plane of the Fisher-KPP equation (2.1.8) and equation (2.1.9) for $c = 0, 0.5, 1, 1.5, 3$ and 10 as shown in Figure 2. Figure 3 indiciates the phase portrait of the travelling waves, the trapping region at $c = 2$ and the corresponding heteroclinic trajectory between $(0,0)$ and $(1,0)$. We observe that the interior of the homoclinic orbit when $c = 0$ in Figure 3 is a trapping region.

We now consider the vector field near $(u,v) = (0,0)$ when $c \neq 0$ along the homoclinic orbit by denoting $F(u,v)$ as:

$$F(u,v) = \begin{pmatrix} u \\ v \end{pmatrix}' = \begin{pmatrix} v \\ -cv - u(1-u) \end{pmatrix}, \tag{2.1.10}$$

We have

$$F(u,v) \cdot \nabla K = \left\langle \begin{pmatrix} v \\ -cv - u(1-u) \end{pmatrix}, \begin{pmatrix} u(1-u) \\ v \end{pmatrix} \right\rangle \tag{2.1.11}$$

$$= -cv^2. \tag{2.1.12}$$

where

$$\nabla K = \left(-u^2 + u, v\right) \tag{2.1.13}$$

$$= (u(1-u), v)\,. \tag{2.1.14}$$

The equation for the homoclinic orbit is found by solving equation (2.1.3), which results in equation (2.1.4). In this case, C in equation (2.1.4) is also the value of the Hamiltonian $K(u, v)$ and $C = 0$ along the homoclinic. Figure 4 is the phase portrait of the standing wave to the Fisher-KPP equation. The locus of the homoclinic orbit forms a trapping region when $c \neq 0$. These results establish the existence of a bounded solution to the travelling waves ODE for $c \geq 0$, which decays to 1 as $z \to -\infty$. Therefore, the travelling wave solution to the PDE exists for every c value.

Now if we choose only the $\mathcal{O}(\epsilon)$ term in equation (2.1.10) where $u = u_0 + \epsilon u_1 + \mathcal{O}(\epsilon^2)$ and $v = v_0 + \epsilon v_1 + \mathcal{O}(\epsilon^2)$, then we obtain the linearisation

$$\begin{pmatrix} u \\ v \end{pmatrix}' = DF(u_0, v_0) \begin{pmatrix} u \\ v \end{pmatrix},$$

where DF is the Jacobian. At the fixed points of equation (2.1.10), we have

$$DF(0,0) = \begin{pmatrix} 0 & 1 \\ -1 & -c \end{pmatrix},$$

and

$$DF(1,0) = \begin{pmatrix} 0 & 1 \\ 1 & -c \end{pmatrix}.$$

According to the Hartman-Grobman theorem [**Gro59**], [**Gro62**], [**Har60**], [**Har63**], let g be the flow (solution) of the non-linear ODE and f is the flow of the linearisation of g at an equilibrium (u_0, v_0), then g solves equation (2.1.10). This implies that f and g are topologically conjugate if there exists a homeomorphism H mapping an open set U containing the origin onto an open set V containing the origin and

$$H^{-1}\left(f\left(H\begin{pmatrix} u \\ v \end{pmatrix}\right)\right) = g\begin{pmatrix} u \\ v \end{pmatrix}.$$

Thus, the behaviour of a dynamical system near the equilibrium point is the same as its linearisation near this equilibrium point if no eigenvalue of the linearisation has a real part equal to zero. This means if the eigenvalues of $DF(u_0, v_0)$ all have non-zero real part, then near the point (u_0, v_0), the solution to equation (2.1.10) will be conjugate to the solutions of:

$$\begin{pmatrix} u \\ v \end{pmatrix}' = DF(u_0, v_0) \begin{pmatrix} u \\ v \end{pmatrix}.$$

The Hartman-Grobman theorem [**Gro59**], [**Gro62**], [**Har60**], [**Har63**] states that near $(1, 0)$, solution to equation (2.1.10) will be conjugate to solutions of:

$$\begin{pmatrix} u \\ v \end{pmatrix}' = \begin{pmatrix} 0 & 1 \\ 1 & -c \end{pmatrix} \begin{pmatrix} u \\ v \end{pmatrix} \quad \text{for } c \neq 0,$$

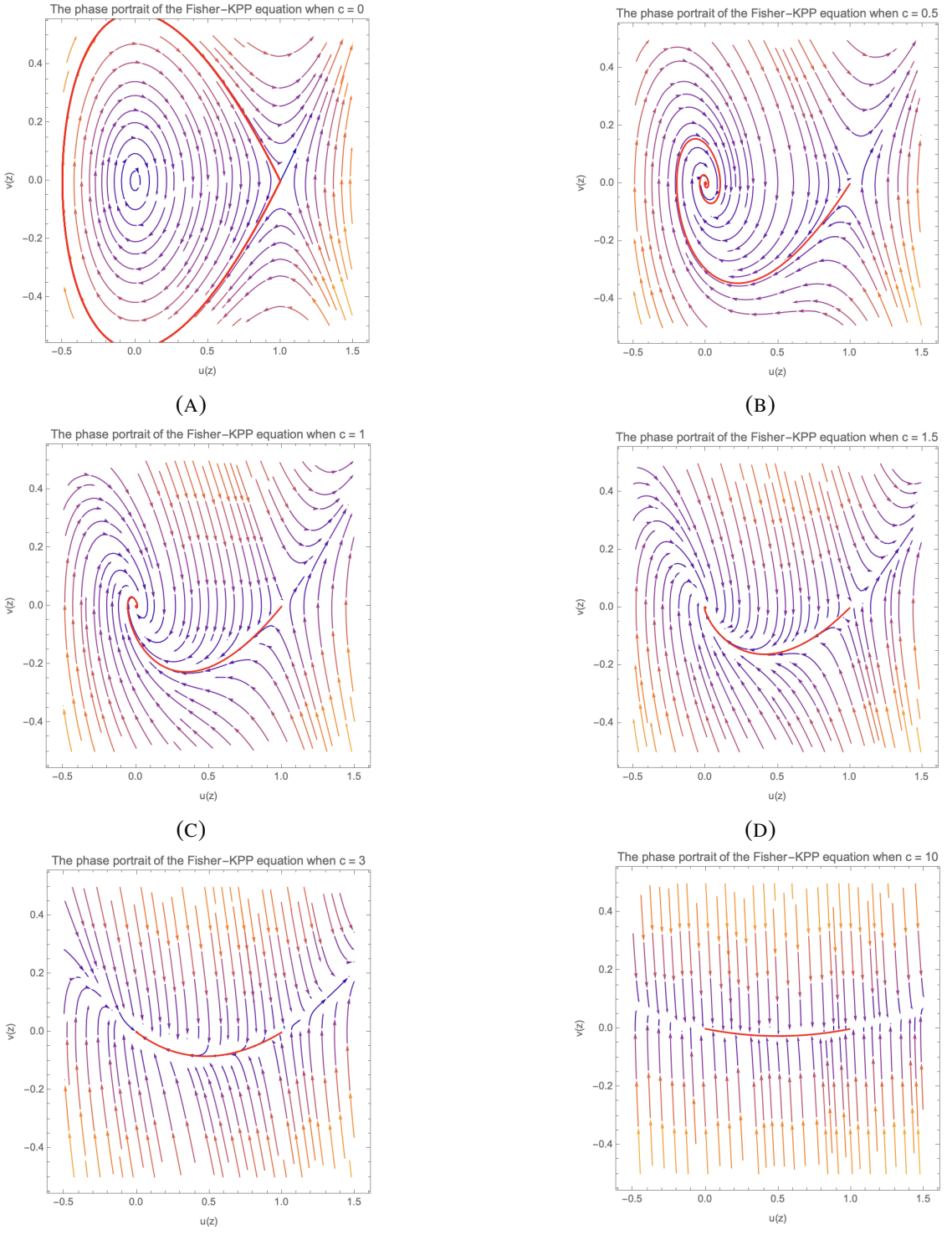

(A) (B) (C) (D) (E) (F)

FIGURE 2. The phase portrait of the Fisher-KPP equation (2.1.8) and equation (2.1.9) when $c = 0, 0.5, 1, 1.5, 3$ and 10. The red curves represent the corresponding heteroclinic trajectories that run between $(0, 0)$ and $(1, 0)$ for each c value. When $c = 0$ in Figure (A), the homoclinic orbit forms a trapping region. When $0 < c < 2$, the heteroclinic orbit approaches (0,0) and then spirals around the origin as seen in Figure (B), (C) and (D). However, when $c \geq 2$, the heteroclinic orbit between two equilibrium points $(0, 0)$ and $(1, 0)$ does not spiral around the origin as seen in Figure (E) and (F).

and near $(0,0)$, the solution to $\begin{pmatrix} u \\ v \end{pmatrix}' = DF(0,0)\begin{pmatrix} u \\ v \end{pmatrix}$ will be conjugate to solutions of:

$$\begin{pmatrix} u \\ v \end{pmatrix}' = \begin{pmatrix} 0 & 1 \\ -1 & -c \end{pmatrix}\begin{pmatrix} u \\ v \end{pmatrix} \text{ for } c \neq 0.$$

At (0,0),

$$\det\begin{pmatrix} -\lambda & 1 \\ -1 & -c-\lambda \end{pmatrix} = 0 \Rightarrow \lambda^2 + c\lambda + 1 = 0.$$

Therefore,

$$\lambda_{\pm} = \frac{1}{2}[-c \pm \sqrt{c^2-4}], \tag{2.1.15}$$

and $(0,0)$ is a stable node for $c \geq 2$ and stable spiral if $0 < c < 2$.

At (1,0),

$$\det\begin{pmatrix} -\lambda & 1 \\ 1 & -c-\lambda \end{pmatrix} = 0 \Rightarrow \lambda^2 + c\lambda - 1 = 0. \tag{2.1.16}$$

Hence,

$$\lambda_{\pm} = \frac{1}{2}[-c \pm \sqrt{c^2+4}], \tag{2.1.17}$$

and $(1,0)$ is a saddle point $\forall c \in \mathbb{R}$.

The existence of solutions can be proved by comparing the eigenvectors of the linearisation around the point $(1,0)$ and $u'(z) = 0$. We have

$$u_1 = \begin{pmatrix} 1 \\ 1 \end{pmatrix}, \tag{2.1.18}$$

and

$$u_2 = \begin{pmatrix} -1 \\ 1 \end{pmatrix}. \tag{2.1.19}$$

At $c \neq 0$, the unstable eigenvector of DF is

$$u_{\mu_+^0} = \begin{pmatrix} 1 \\ \mu_+^0 \end{pmatrix}. \tag{2.1.20}$$

For $c \geq 0$, the slope of this line is

$$\mu_+^0 = \frac{1}{2}\left(-c + \sqrt{c^2+4}\right) \text{ for } -1 < \mu_+^0 \leq 1. \tag{2.1.21}$$

We also notice that $\mu_+^0 > 0$ and $\mu_+^0\Big|_{c=0} = 1$, and

$$\frac{d}{dc}\mu_+^0 = \frac{1}{2}\left(-1 + \frac{c}{\sqrt{c^2+4}}\right) < 0. \tag{2.1.22}$$

This result indicates $\mu_-^0 = \frac{1}{2}\left(-c - \sqrt{c^2+4}\right)$ always decreases with increasing c. Hence, the maximum value of the slope is at $c = 0$. For $c \neq 0$, the part of the unstable manifold with $v > 0$ is inside the homoclinic orbit and the entire solution in the phase plane lies within the homoclinic orbit of the speed $c = 0$. This implies that the homoclinic orbit in the standing wave phase plane is the boundary of a trapping region. Therefore, there is a travelling wave solution decaying to 1 as $z \to -\infty$.

Moreover, from the phase portrait of the travelling waves to the Fisher-KPP equation (2.1.8) and equation (2.1.9) as shown in Figure 3 and the phase portrait of the standing wave to the Fisher-KPP equation (2.1.10) as shown in Figure 4, we observe that the relevant heteroclinic trajectory from the saddle point $(1, 0)$ never leaves that region and thus, by LaSalle's invariance principle [**Mei07**], the trajectory must end at the stable node $(0, 0)$.

Theorem 2.1.1. *According to LaSalle's invariance principle in* [**Mei07**]*, suppose that L is a weak-Lyapunov function on some compact, forward-invariant neighbourhood U of the equilibrium point* $(1, 0)$*. Let $Z = \{\frac{dL}{dz} = 0\}$ for equilibrium points in U be the set where L is not decreasing. Then if the equilibrium point is the largest forward invariant subset of Z, it is asymptotically stable and attracts every point in U.*

The calculation in equation (2.1.13) shows that K is a weak-Lyapunov function and $Z = \{\frac{dL}{dz} = 0\}$ is just the set $(0, 0)$.

In this section, we considered constant solutions at two fixed points $u = 0$ and $u = 1$ in equation (1.0.5). We have also established that $u = 0$ is unstable in time and stable in space whereas $u = 1$ is stable in time and unstable in space for travelling waves problem. Moreover, we looked at the vector field near $(u, v) = (0, 0)$ and the behaviour of the dynamical system near the equilibrium points. We have found that $(0, 0)$ is a stable node for $c \geq 2$ and stable spiral if $0 < c < 2$ whereas $(1, 0)$ is a saddle point. We also showed the existence of solutions by constructing a trapping region in the plane for the orbit of the Fisher-KPP equation and comparing the eigenvectors of the linearisation around 0 at $c = 0$.

2.2. Stability of standing waves in the Fisher-KPP equation

Now, we view the Fisher-KPP equation (1.0.5) as a dynamical system on an infinite dimensional space by letting

$$\dot{u} = \mathcal{F}(u), \tag{2.2.1}$$

where $\dot{u} := \partial_t u$ and $\mathcal{F}(u) = u_{xx} + u(1 - u)$.

A standing wave solution to equation (1.0.5) is one depending on x only. Let us consider the solution at h by solving:

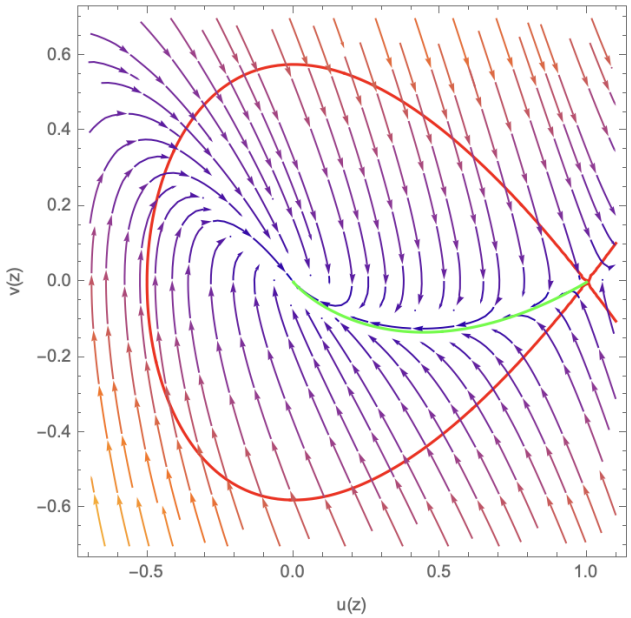

FIGURE 3. The phase portrait of the travelling waves of the Fisher-KPP equation (2.1.8) and equation (2.1.9), the trapping region when the wave speed $c = 2$ and the corresponding heteroclinic trajectory between the two equilibrium points $(0, 0)$ and $(1, 0)$. The red curve represents a homoclinic orbit when $c = 0$ and it is the boundary of a trapping region. The green curve indicates a heteroclinic trajectory that runs between $(1, 0)$ and $(0, 0)$ when $c > 0$. Asymptotically the wave lies within the trapping region then decays to 1 as $z \to -\infty$.

$$h_{xx} + h(1 - h) = 0, \tag{2.2.2}$$

where $h(x)$ is a fixed point of equation (2.2.1) as $\mathcal{F}(h) = 0$.

If we impose boundary conditions

$$h(+\infty) = h(-\infty) = 0, \tag{2.2.3}$$

such a solution to equation (2.2.2) can be explicitly described by the following formula:

$$h(x) = 1 - \frac{3}{2}\text{sech}^2\left(\frac{x}{2}\right) \tag{2.2.4}$$

The plot of solution $h(x)$ described in equation (2.2.4) in the phase plane of equation (2.1.10) is shown in Figure 4.

In ordinary dynamical systems, we focus on $DF(x_*)$ which is the Jacobian of the fixed point and the eigenvalues. Since we do not have a Jacobian for $\mathcal{F}$, we consider the linear part of $\mathcal{F}$ as an operator which acts on the direction of perturbation. We look at $\mathcal{F}(h+\epsilon p(x))$ and keep the $\mathcal{O}(\epsilon)$ term to obtain an operator that acts on p as follows

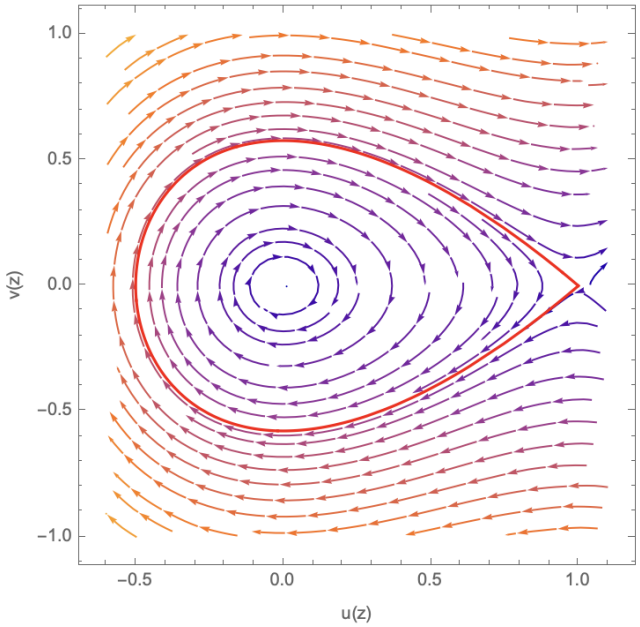

FIGURE 4. The phase portrait of the standing wave of the Fisher-KPP equation (2.1.10). The red curve represents the plot of solution $h(x)$ described in equation (2.2.4) in the phase plane of equation (2.1.10). The locus of the homoclinic orbit forms a trapping region for the heteroclinic orbit when $c \neq 0$.

$$\mathcal{F}(h+\epsilon p) = \mathcal{F}(h) + \epsilon L p + \mathcal{O}(\epsilon^2) \tag{2.2.5}$$

$$= (h+\epsilon p)_{xx} + (h+\epsilon p)(1-h-\epsilon p) \tag{2.2.6}$$

$$= h_{xx} + h(1-h) + \epsilon(p_{xx} + (1-2h)p) - \epsilon^2 p^2, \tag{2.2.7}$$

where p is the perturbation of the function $h(x)$.

Thus, L is the linear operator given by

$$Lp := \lim_{\epsilon \to 0} \frac{\partial}{\partial \epsilon} \mathcal{F}(h+\epsilon p) = p_{xx} + (1-2h(x))p. \tag{2.2.8}$$

We now consider the linear differential equation

$$p_t = Lp = p_{xx} + (1-2h(x))p. \tag{2.2.9}$$

Equation (2.2.9) indicates how p's that start "near" h evolve in time under the influence of $\mathcal{F}$ for the short-term. Since we want the perturbation p to be "near" h, this requires ϵp to be "near" h so the following is satisfied:

$$\sqrt{\int_{\mathbb{R}} [h-(h+\epsilon p)]^2 dx} \ll 1$$

$$\implies \epsilon\sqrt{\int_{\mathbb{R}} p^2 dx} \ll 1. \tag{2.2.10}$$

Since we can pick ϵ as small as we need, equation (3.2.10) is equivalent to:

$$\int p^2 dx < \infty.$$

The number λ is called an eigenvalue and the corresponding p is called the eigenfunction. If $Re(\lambda) > 0$, then h is an unstable fixed point of equation (1.0.5). Thus, we define $p \in L^2(\mathbb{R})$ to be "near" h if and only if it has a finite square integral.

We say that $\lambda \in \mathbb{C}$ is in the spectrum of L if $L - \lambda I$ is not an invertible operator and write $\lambda \in \sigma(L)$. We would like to know the spectrum by finding $\lambda \in \mathbb{C}$ such that $L - \lambda I$ is not invertible. In inifite dimensions, a linear operator L is not invertible if and only if it is not one-to-one or not onto [**KP13**].

Definition 2.2.1. According to Kapitula and Promislow [**KP13**], we let X be a Banach space and let $L : \tilde{D}(L) \subset X \to X$ be a closed linear operator with domain $\tilde{D}(L)$ dense in X. The operator L is Fredholm operator if
(a) $\ker(L)$ is finite-dimensional,
(b) $R(L)$ is closed with finite codimension where $R(L)$ denotes the range of L.
Hence, the spectrum of L consists of the following two sets:
(1) The essential spectrum of a Fredholm operator L, $\sigma_{ess}(L)$, is the set of all $\lambda \in \mathbb{C}$ such that either $\lambda I - L$ is not Fredholm, or $\lambda I - L$ is Fredholm, but $\text{ind}(\lambda I - L) \neq 0$.
(2) The point spectrum of a Fredholm operator L is the set defined by

$$\sigma_{pt}(L) = \lambda \in \mathbb{C} : \text{ind}(\lambda I - L) = 0, \text{ but } \lambda I - L \text{ is not invertible.}$$

The elements of the point spectrum are called eigenvalues of L. The equivalent definition of Fredholm operator and index can also be found in Section 2.2.5 of [**KP13**].

In our case, $\partial_x - A$ is Fredholm if $\text{Re}(\sigma(A)) \neq 0$ and the index of an operator of the form $(\partial_x - A)$ for $A \in M_n(\mathbb{R})$ is written as $\text{ind}(\partial_x - A)$ which denotes the number of negative eigenvalues of A.

Theorem 2.2.1. *According to* [**KP13**]*, the operator L is a relatively compact perturbation of L_0 if $(L_0 - L)(\lambda I - L_0)^{-1} : X \to X$ is compact for some $\lambda \in \sigma(L_0)$. The stability theorem for relatively compact perturbations of Fredholm operators is also referred to as Weyl's essential spectrum theorem in* [**KP13**]*. By letting L and L_0 be closed linear operators in a Banach space X, if L is a relatively compact perturbation of L_0 then:*
(1) The operator $\lambda I - L$ is Fredholm if and only if $\lambda I - L_0$ is Fredholm.
(2) $ind(\lambda I - L) = ind(\lambda I - L_0)$.
(3) The operator L and L_0 have the same essential spectra. In particular, $\sigma_{ess}(L) = \sigma_{ess}(L_0)$.

The operator $L\mathcal{F}(h)-\lambda$ will not be one-to-one if there exists $p \neq 0$ such that $(L\mathcal{F}(h)-\lambda)p = 0$. In particular, if we can find a $\lambda \in \sigma(L)$ so that $Re(\lambda) > 0$ and there is a solution to

$$p_{xx} + (1 - 2h(x))p = \lambda p. \tag{2.2.11}$$

In order to determine the invertability of L, we will construct a Green's function. We want to solve

$$(L - \lambda)p = \delta(x - y). \tag{2.2.12}$$

The right hand side of equation (2.2.12) is the Dirac δ function and is defined according to three following conditions[**Gri02**]:

$$\delta(x) = 0 \text{ unless } x = 0,$$

$$\int_{\mathbb{R}} \delta(x)dx = 1,$$

and

$$\int_{\mathbb{R}} f(x)\delta(x - a)dx = f(a) \text{ for any } f \in C_0^\infty(\mathbb{R}),$$

One way to view the Dirac δ function is as the limit of the sequence of functions:

$$d_n(x) = \frac{n}{\pi(1 + (nx)^2)}, \tag{2.2.13}$$

and

$$\delta(x) = \lim_{n\to\infty} d_n(x).$$

From Figure 5, $d_n(x)$ will become sharper as $n \to \infty$, but the integral value is always equal to 1.

Suppose we can find a solution $G_\lambda(x, y)$ to $(L-\lambda)G_\lambda(x, y) = \delta(y-x)$ for a given value of λ and any $y \in \mathbb{R}$. By applying $(L - \lambda)$ on both sides, the solution of $(L - \lambda)p = f$ can be found as following:

$$(L - \lambda)p = (L - \lambda)\int G_\lambda(x, y)f(y)dy \tag{2.2.14}$$

$$= \int (L - \lambda)G_\lambda(x, y)f(y)dy \tag{2.2.15}$$

$$= \int \delta(y - x)f(y)dy \tag{2.2.16}$$

$$= f(x). \tag{2.2.17}$$

(2.2.18)

Here we call $G_\lambda(x, y)$ a Green's function.

We observe that for a given fixed $y \in \mathbb{R}$ unless $x = y$, $G_\lambda(x, y)$ is a solution to

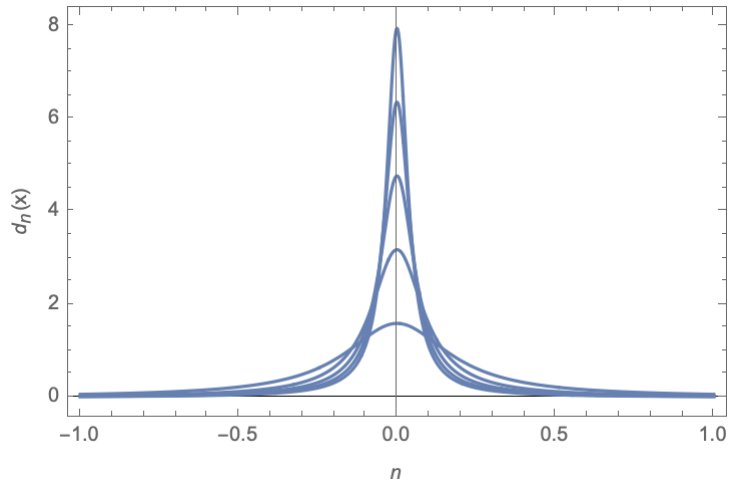

FIGURE 5. A plot of $d_n(x)$ in equation (2.2.13) for various values of n. In this case, $d_n(x)$ becomes sharper as $n \to \infty$. However, the integral value is always equal to 1.

$$(L - \lambda)G_\lambda(x, y) = 0.$$

We also want $G_\lambda(x, y) \in L^2(\mathbb{R})$, then $G_\lambda(x, y)$ must decay to 0 as $x \to \pm\infty$. By looking at the far-field solutions $\lim_{x\to\pm\infty}$ to $(L - \lambda)p = 0$ at a fixed $y \in \mathbb{R}$, we observe that $\lim_{x\to\pm\infty} h(x) = 0$. Hence, from equation (2.2.11), the general solution to

$$p_{xx} - (\lambda + 1)p = 0 \tag{2.2.19}$$

is

$$p = c_1 e^{-x\sqrt{\lambda+1}} + c_2 e^{x\sqrt{\lambda+1}}.$$

If the far-field operator does not contain solutions which decay to 0, then we cannot find a Green's function. We conclude that the operator L is not Fredholm when $\lambda < -1$. Thus, the essential spectrum of L consists of the set $(-\infty, -1]$. Now, we look at solutions of equation (2.2.11) where $\lambda > -1$ so that there exists solutions $p = ce^{x\sqrt{\lambda+1}}$ which decay to 0 as $x \to \pm\infty$.

2.2.1. Point spectrum of the standing waves.

First we establish that L has only real eigenvalues. Integrating by parts twice, for v and $\bar{v}$ are arbitrary and functions in L^2, we have:

$$\int v_{xx}\bar{v}dx = v_x\bar{v}\Big|_{-\infty}^{\infty} - \int v_x\bar{v}_x dx \tag{2.2.20}$$

$$= -\bar{v}_x v\Big|_{-\infty}^{\infty} + \int v\bar{v}_{xx}dx \tag{2.2.21}$$

$$= \int v\bar{v}_{xx}dx. \tag{2.2.22}$$

Hence,

$$\int (v_{xx} + (1-2h)v)\bar{v}dx = \int v(\bar{v}_{xx} + (1-2h)\bar{v})dx \tag{2.2.23}$$

$$= \int vL\bar{v}dx. \tag{2.2.24}$$

As a consequence,

$$\int_{\mathbb{R}} Lv\bar{v}dx = \int_{\mathbb{R}} vL\bar{v}dx$$

If λ is an eigenvalue of L

$$\implies \lambda \int_{\mathbb{R}} v\bar{v}dx = \bar{\lambda} \int_{\mathbb{R}} v\bar{v}dx.$$

This implies that $\lambda = \bar{\lambda}$ or $\lambda \in \mathbb{R}$.

We now look for a solution to equation (2.2.11) which decays to 0 as $x \to -\infty$. Let us call this decaying solution as $p_U(x;\lambda)$. Using Mathematica, we can compute the solution of equation (2.2.11) using $h(x)$ as given by equation (2.2.4) to be

$$p_U(x,\lambda) = e^{\sqrt{\lambda+1}x}\left(-\frac{8}{15}\lambda\sqrt{\lambda+1} + \frac{1}{5}(8\lambda+5)\tanh\left(\frac{x}{2}\right) - 2\sqrt{\lambda+1}\tanh^2\left(\frac{x}{2}\right) + \tanh^3\left(\frac{x}{2}\right)\right).$$

We also use Mathematica to compute the solution of equation (2.2.11) which decays at $x \to +\infty$ and let us call this solution as $p_S(x;\lambda)$:

$$p_S(x,\lambda) = e^{\sqrt{\lambda+1}(-x)}\left(\frac{8}{15}\lambda\sqrt{\lambda+1} + \frac{1}{5}(8\lambda+5)\tanh\left(\frac{x}{2}\right) + 2\sqrt{\lambda+1}\tanh^2\left(\frac{x}{2}\right) + \tanh^3\left(\frac{x}{2}\right)\right).$$

By setting $q := p_x$, we can solve equation (2.2.11) as the linear system of equations:

$$\begin{pmatrix} p \\ q \end{pmatrix}_x = \begin{pmatrix} 0 & 1 \\ \lambda - 1 + 2h(x) & 0 \end{pmatrix}\begin{pmatrix} p \\ q \end{pmatrix}. \tag{2.2.25}$$

We observe that from continuous spectrum, for $\lambda > -1$, if these solutions agree for a single x, then due to the linearity of the system in equation (2.2.25), they must agree for all $x \in \mathbb{R}$. Therefore, we choose $x = 0$ to examine whether these solutions agree for a single x by evaluating the determinant

$$D(\lambda) = \begin{vmatrix} p_U(0;\lambda) & p_S(0;\lambda) \\ (p_U)_x(0;\lambda) & (p_S)_x(0;\lambda) \end{vmatrix} \tag{2.2.26}$$

$$= \frac{8}{225}(\sqrt{\lambda+1})\lambda(4\lambda-5)(4\lambda+3). \tag{2.2.27}$$

If $\lambda > -1$ and $D(\lambda) = 0$, the columns of the matrix are dependent. This implies that $p_U = kp_S$ for all $x \in \mathbb{R}$. Therefore, $p_U(x;\lambda) = p_S(x;\lambda)$. This must be an eigenfunction and λ must be an eigenvalue. Thus, the spectrum of the operator L is the set

$$\sigma(L) := (-\infty,-1] \cup \left\{\frac{-3}{4}\right\} \cup \{0\} \cup \left\{\frac{5}{4}\right\}.$$

We observe that the wave $h(x)$ is not stable and the linear operator L has three eigenvalues and other values λ where the operator is not invertible.

By using Mathematica and looking at the eigenfunctions for the three eigenvalues:

$$\hat{p_2}\left(x;-\frac{3}{4}\right) = \frac{1}{5}(-3+2\cosh(x))\operatorname{sech}^3\left(\frac{x}{2}\right),$$

$$\hat{p_1}(x;0) = 8\operatorname{csch}^3(x)\sinh^4\left(\frac{x}{2}\right) = -\frac{3}{2}h_x(x),$$

and

$$\hat{p_0}\left(x;\frac{5}{4}\right) = \operatorname{sech}^3\left(\frac{x}{2}\right),$$

we can see that $\lambda_0 > \lambda_1 > \lambda_2$.

By using Mathematica, our normalised eigenfunctions are

$$p_2\left(x;-\frac{3}{4}\right) = \sqrt{\frac{75}{32}} \times \frac{1}{5}(-3+2\cosh(x))\operatorname{sech}^3\left(\frac{x}{2}\right) \tag{2.2.28}$$

$$= \frac{\sqrt{6}}{8}(-3+2\cosh(x))\operatorname{sech}^3\left(\frac{x}{2}\right), \tag{2.2.29}$$

$$p_1(x;0) = \sqrt{\frac{15}{8}} \times 8\operatorname{csch}^3(x)\sinh^4\left(\frac{x}{2}\right) \tag{2.2.30}$$

$$= 2\sqrt{30}\operatorname{csch}^3(x)\sinh^4\left(\frac{x}{2}\right), \tag{2.2.31}$$

and

$$p_0\left(x;\frac{5}{4}\right) = \sqrt{\frac{15}{32}}\operatorname{sech}^3\left(\frac{x}{2}\right) \tag{2.2.32}$$

$$= \frac{\sqrt{30}}{8}\operatorname{sech}^3\left(\frac{x}{2}\right). \tag{2.2.33}$$

These eigenfunctions characterise the behaviour of the set of eigenvalues as stated in the theory of Kapitula and Promislow [**KP13**].

According to theorem 2.3.2 in Kapitula and Promislow [**KP13**], the point spectrum, $\sigma_{\text{pt}}(L)$, contains a finite number, possibly zero, of simple eigenvalues, which can be enumerated in a strictly descending order

$$\lambda_0 > \lambda_1 > \lambda_2 > -1 := \max\{-1,-1\}. \tag{2.2.34}$$

For $j = 0, 1$ and 2, the eigenfunction $p_j(x)$ associated with the eigenvalue λ_j can be normalised so that p_j has j simple zeroes and the eigenfunctions are orthonormal.

2.3. Stability of travelling waves in the Fisher-KPP equation

In this section, we look at solutions of $u(x,t) = v(z,t)$ which solve:

$$v_t = v_{zz} + cv_z + v(1-v). \tag{2.3.1}$$

For a fixed $v(z,t) = v_c(z)$ which solves equation (2.1.6) and the set of boundary conditions in equation (2.1.7), we linearise equation (2.3.1) about $v_c(z)$:

$$v = v_c(z) + \epsilon p(z,t). \tag{2.3.2}$$

Substituting equation (2.3.2) into equation (2.3.1) and keeping $\mathcal{O}(\epsilon)$ terms, we obtain:

$$p_t = p_{zz} + cp_z + (1 - 2v_c(z))p \tag{2.3.3}$$

$$= L(v_c(z))p. \tag{2.3.4}$$

We look for $\lambda \in \mathbb{C}$ such that $\mathcal{L}(v_c(z)) - \lambda$ is not invertible by writing:

$$L(v_c(z))p - \lambda p = p_{zz} + cp_z + (1 - 2v_c(z))p - \lambda p$$

as a system:

$$\begin{pmatrix} p \\ q \end{pmatrix}_z = \begin{pmatrix} 0 & 1 \\ \lambda - 1 + 2v_c & -c \end{pmatrix} \begin{pmatrix} p \\ q \end{pmatrix} =: A(z;\lambda) \begin{pmatrix} p \\ q \end{pmatrix}, \tag{2.3.5}$$

where $q = p_z$. To find a Green's function in $L^2(\mathbb{R})$, we need to have decaying solutions in the far-field. If

$$\lim_{z \to -\infty} v_c(z) = 1, \tag{2.3.6}$$

and

$$\lim_{z \to +\infty} v_c(z) = 0, \tag{2.3.7}$$

then as $z \to -\infty$, equation (2.3.5) becomes:

$$\begin{pmatrix} p \\ q \end{pmatrix}_z = \begin{pmatrix} 0 & 1 \\ \lambda + 1 & -c \end{pmatrix} \begin{pmatrix} p \\ q \end{pmatrix} =: A_-(\lambda) \begin{pmatrix} p \\ q \end{pmatrix}, \tag{2.3.8}$$

and as $z \to +\infty$, equation (2.3.5) becomes:

$$\begin{pmatrix} p \\ q \end{pmatrix}_z = \begin{pmatrix} 0 & 1 \\ \lambda - 1 & -c \end{pmatrix} \begin{pmatrix} p \\ q \end{pmatrix} =: A_+(\lambda) \begin{pmatrix} p \\ q \end{pmatrix}. \tag{2.3.9}$$

2.3.1. The asymptotic operator and the essential spectrum.

We would like to examine the constant coefficient system:

$$\begin{pmatrix} p \\ q \end{pmatrix}_z = \begin{cases} A_- \begin{pmatrix} p \\ q \end{pmatrix} & \text{for } z < 0. \\ A_+ \begin{pmatrix} p \\ q \end{pmatrix} & \text{for } z > 0. \end{cases} \tag{2.3.10}$$

This comes from the non-continuous but constant coefficient (asymptotic) operator:

$$L_\infty := \partial_{zz} + c\partial_z \mp 1. \tag{2.3.11}$$

According to Weyl's essential spectrum theorem in Kapitula and Promislow [**KP13**], any essential spectrum of L_∞ will be the same as the essential spectrum of L, $\sigma_{\text{ess}}(L_\infty) = \sigma_{\text{ess}}(L)$.

Equation (2.3.8) has the general solution:

$$\begin{pmatrix} p \\ q \end{pmatrix} = c_1 e^{\alpha_-(\lambda)z} \begin{pmatrix} 1 \\ \alpha_-(\lambda) \end{pmatrix} + c_2 e^{\alpha_+(\lambda)z} \begin{pmatrix} 1 \\ \alpha_+(\lambda) \end{pmatrix}, \tag{2.3.12}$$

where $\alpha_\pm(\lambda)$ are the eigenvalues of the matrix $A_-(\lambda)$.

The eigenvalues of $A_-(\lambda)$ will be

$$\det(A - \alpha) = \alpha^2 + c\alpha - \lambda - 1 = 0 \tag{2.3.13}$$

$$\implies \alpha_\pm(\lambda) = \frac{1}{2}\left(-c \pm \sqrt{c^2 + 4(\lambda + 1)}\right) \tag{2.3.14}$$

Equation (2.3.9) has the general solution:

$$\begin{pmatrix} p \\ q \end{pmatrix} = d_1 e^{\omega_-(\lambda)z} \begin{pmatrix} 1 \\ \omega_-(\lambda) \end{pmatrix} + d_2 e^{\omega_+(\lambda)z} \begin{pmatrix} 1 \\ \omega_+(\lambda) \end{pmatrix}, \tag{2.3.15}$$

where $\omega_\pm(\lambda)$ are the eigenvalues of the matrix $A_+(\lambda)$.

The eigenvalues of $A_+(\lambda)$ will be solutions to

$$\det(A - \omega) = \omega^2 + c\omega - \lambda + 1 = 0. \tag{2.3.16}$$

$$\implies \omega_\pm(\lambda) = \frac{1}{2}\left(-c \pm \sqrt{c^2 + 4(\lambda - 1)}\right). \tag{2.3.17}$$

We are going to invert operator $\mathcal{L}$ in equation (2.3.11) by finding decaying solutions to the equation (2.3.12) and equation (2.3.15) which are parametrised by λ. We begin with

a real $\lambda \gg 1$ at $\alpha_{\pm}(\lambda)$ and $\omega_{\pm}(\lambda)$. Our observation is that $\alpha_{-}(\lambda) > 0$ while $\alpha_{+}(\lambda) < 0$ and $\omega_{-}(\lambda) > 0$ while $\omega_{+}(\lambda) < 0$. As a result, we can see that part of the solution to equation (2.3.12) corresponds to $\alpha_{+}(\lambda)$ decays as $z \to +\infty$ and the solution corresponding to $\omega_{-}(\lambda)$ decays as $z \to -\infty$. At $z = 0$, there are two solutions:

$$\xi_u(0) := c_2 \begin{pmatrix} 1 \\ \alpha_{-}(\lambda) \end{pmatrix},$$

and

$$\xi_s(0) := d_1 \begin{pmatrix} 1 \\ \omega_{+}(\lambda) \end{pmatrix}.$$

In order to invert the constant coefficient operator L in equation (2.3.11) and find values for c_2 and d_1, we need to solve $(L_\infty - \lambda)p = \delta x$. This means we will find c_2 and d_1 so that:

$$\begin{pmatrix} 1 & -1 \\ \alpha_{-}(\lambda) & -w_{+}(\lambda) \end{pmatrix} \begin{pmatrix} c_2 \\ d_1 \end{pmatrix} = \begin{pmatrix} 0 \\ -1 \end{pmatrix}. \tag{2.3.18}$$

Solving equation (2.3.18) gives:

$$c_2 = \frac{1}{\omega_{+}(\lambda) - \alpha_{-}(\lambda)},$$

and

$$d_1 = \frac{1}{\alpha_{-}(\lambda) - \omega_{+}(\lambda)}.$$

Next, we look at the values of λ so that the real parts of $\alpha_{\pm}$ and $\omega_{\pm}$ vanish. By letting $k \in \mathbb{R}$, we solve $\det(A_{\pm} - ik) = 0$ to obtain

$$\lambda_{\pm} = -k^2 \pm 1 + ick. \tag{2.3.19}$$

We define Ω_1, Ω_2 and Ω_3 in Figure 6 as following:

$$\Omega_1 : \operatorname{ind}(\partial_x - A_{+}(\lambda)) = 2 \text{ and } \operatorname{ind}(\partial_x - A_{-}(\lambda)) = 2, \tag{2.3.20}$$

$$\Omega_2 : \operatorname{ind}(\partial_x - A_{+}(\lambda))) = 1 \text{ and } \operatorname{ind}(\partial_x - A_{-}(\lambda)) = 2, \tag{2.3.21}$$

and

$$\Omega_3 : \operatorname{ind}(\partial_x - A_{+}(\lambda)) = \operatorname{ind}(\partial_x - A_{-}(\lambda)) = 1. \tag{2.3.22}$$

Equation (2.3.19) represents a pair of parametrised parabolas that open leftwards in the complex plane with vertices at ± 1 and the parametric variable k is the imaginary part of the eigenvalue $A_{\pm}(\lambda)$ as seen in Figure 6. Therefore, for λ to the right of both curves, we have that the signature of $A_{\pm}(\lambda)$ is $(-1, 1)$ (both $A_{+}(\lambda)$ and $A_{-}(\lambda)$ have one negative eigenvalue and one positive eigenvalue). For λ to the left, we have $A_{\pm}(\lambda)$ is $(-1, -1)$ (both $A_{+}(\lambda)$ and $A_{-}(\lambda)$ have two negative eigenvalues). Along the red curve, $A_{+}(\lambda)$ has signature (0,-1). Along the blue curve, $A_{-}(\lambda)$ has signature (0,-1). In between the two curves, we have that $A_{+}(\lambda)$ has signature $(1, -1)$ ($A_{+}(\lambda)$ has one negative eigenvalue and one positive eigenvalue) while $A_{-}(\lambda)$ has signature $(-1, -1)$ ($A_{-}(\lambda)$ has two negative eigenvalues).

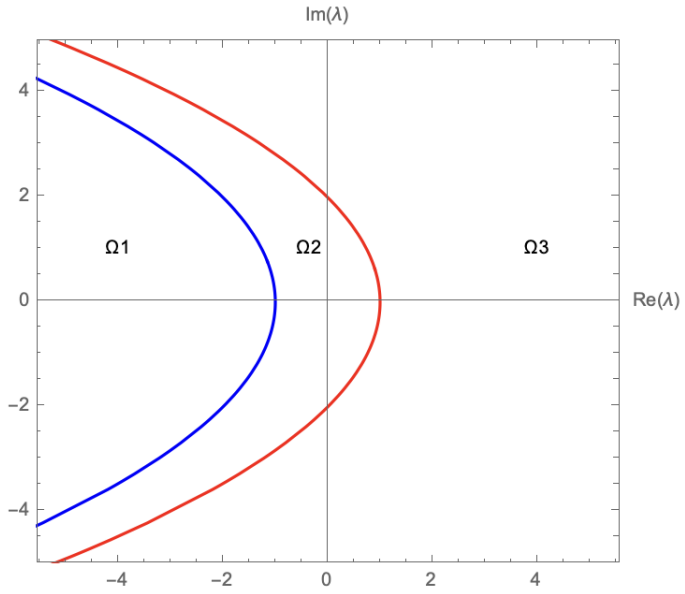

FIGURE 6. The essential spectrum of a travelling wave in the Fisher-KPP model is the set bounded by the two parabolas in equation (2.3.19). These parabolas open leftwards in the complex plane with vertices at ± 1. The parametric variable $k \in \mathbb{R}$ is the imaginary part of the eigenvalue $A_{\pm}(\lambda)$. The regions Ω_1, Ω_2 and Ω_3 are defined in equations (2.3.20) to (2.3.22). The blue curve is the set of $\lambda \in \mathbb{C}$ where $A_{-}(\lambda)$ has purely imaginary eigenvalue and the red curve is the set where $A_{+}(\lambda)$ has a purely imaginary eigenvalue. For λ to the right of both curves, i.e. in Ω_3, $A_{\pm}(\lambda)$ has signature $(-1, 1)$. For λ to the left, i.e. in Ω_1, $A_{\pm}(\lambda)$ has signature $(-1, -1)$. On the red curve, the signature of $A_{+}(\lambda)$ is (0,-1). On the blue curve, the signature of $A_{-}(\lambda)$ is (0,-1). In between these two curves, the signature of $A_{+}(\lambda)$ is $(1, -1)$ ($A_{+}(\lambda)$ and the signature of $A_{-}(\lambda)$ is $(-1, -1)$.

In this case, signature of a matrix as tripe of integers $\left(u_{-}, u_{+}, u_{0}\right)$ counting the number of eigenvalues with negative, positive and zero real part respectively. The convention is to drop u_0 if the matrix is hyperbolic.

Since $\alpha_{+}(\lambda) \neq \omega_{-}(\lambda)$ for $\lambda \in \mathbb{C}$, we can write the Green's function for $\lambda \in \Omega_3$ of equation (2.3.18) as:

$$G(z, \zeta; \lambda) = \begin{cases} c_2 e^{\alpha_{-}(\lambda)(z-\zeta)} \begin{pmatrix} 1 \\ \alpha_{-}(\lambda) \end{pmatrix} & \text{for } z \leq \zeta, \\ d_1 e^{\omega_{+}(\lambda)(z-\zeta)} \begin{pmatrix} 1 \\ \omega_{+}(\lambda) \end{pmatrix} & \text{for } z \geq \zeta. \end{cases}$$

This result implies that we can find a Green's function of the form

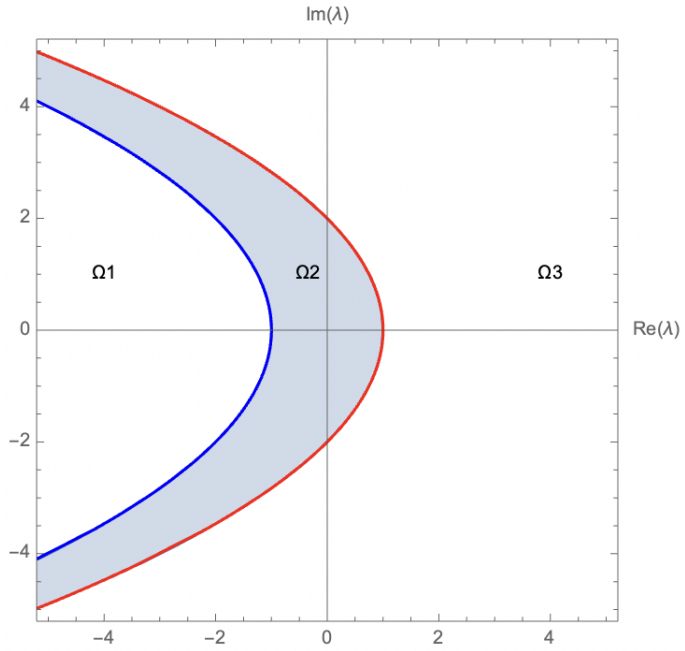

FIGURE 7. The signature of $A_+(\lambda)$ changes along the red curve, and the signature of $A_-(\lambda)$ changes along the blue curve. For λ values between these two curves, as $z \to -\infty$, $A_+(\lambda)$ has two decaying solutions. Hence, based on definition 2.2.1, $L_\infty - \lambda$ is not invertible for λ between these two curves.

$$G(z,\zeta;\lambda) = \begin{cases} 0 \text{ for } z \le \zeta, \\ d_1 e^{\omega_-(\lambda)(z-\zeta)} \begin{pmatrix} 1 \\ \omega_-(\lambda) \end{pmatrix} + d_2 e^{\omega_+(\lambda)(z-\zeta)} \begin{pmatrix} 1 \\ \omega_+(\lambda) \end{pmatrix} \text{ for } z \ge \zeta, \end{cases}$$

where d_i are the solutions of the following system

$$\begin{pmatrix} 1 & 1 \\ \omega_-(\lambda) & \omega_+(\lambda) \end{pmatrix} \begin{pmatrix} d_1 \\ d_2 \end{pmatrix} = \begin{pmatrix} 0 \\ -1 \end{pmatrix}.$$

The solutions exist given the condition that $\omega_+(\lambda) \neq \omega_-(\lambda)$, i.e. except at $\lambda = 1 - \frac{c^2}{4}$. It turns out that such a case, the general solution has the form of

$$\begin{pmatrix} p \\ q \end{pmatrix} = e^{\frac{-cz}{2}} \begin{pmatrix} 1 + \frac{cz}{2} & z \\ \frac{-c^2 z}{4} & 1 - \frac{cz}{2} \end{pmatrix} \begin{pmatrix} d_1 \\ d_2 \end{pmatrix}. \tag{2.3.23}$$

This means that the operator $L_\infty - \lambda$ is invertible for any λ not between the red and blue curves in Figure 6 and Figure 7 (the closure of Ω_2).

Looking at the values of λ between these two curves in Figure 7, we have as $z \to -\infty$, $A_+(\lambda)$ has two decaying solutions. Therefore, according to definition 2.2.1, we conclude

that for λ between these two curves, $\mathcal{L}_\infty - \lambda$ is not invertible and we can find a solution which decays as $z \to \pm\infty$ by solving for d_1 and d_2:

$$\begin{pmatrix} 1 & 1 \\ \omega_-(\lambda) & \omega_+(\lambda) \end{pmatrix} \begin{pmatrix} d_1 \\ d_2 \end{pmatrix} = \begin{pmatrix} 1 \\ \alpha_+(\lambda) \end{pmatrix}.$$

2.3.2. Point spectrum of the travelling waves.

We look for a $\lambda \in \Omega_3$ to the right of the essential spectrum so that

$$L(v_c)p = \lambda p \text{ with } p \in L^2(\mathbb{R}). \tag{2.3.24}$$

Suppose we had an eigenvalue λ to $L(v_c)$ for some λ to the right of the two parabolas in Figure 7. We have a solution p which satisfies $Lp = \lambda p$ where p is in $L^2(\mathbb{R})$. Since p decays, if there exists $p \to 0$ as $z \to \pm\infty$, then

$$\lim_{z\to-\infty} p \sim e^{z\left(\frac{-c}{2}+\sqrt{\lambda+1+\frac{c^2}{4}}\right)},$$

and

$$\lim_{z\to+\infty} p \sim e^{z\left(\frac{-c}{2}-\sqrt{\lambda-1+\frac{c^2}{4}}\right)}.$$

We now look at functions of the form

$$\tilde{q} = e^{\frac{c}{2}z}p,$$

so that

$$p = e^{-\frac{c}{2}z}\tilde{q},$$

then if $p \in L^2\mathbb{R}$, we must have

$$\int_{\mathbb{R}} e^{-cz}\tilde{q}^2 dz < \infty,$$

and if $\tilde{q} \in L^2$, then we must have

$$\int p^2 e^{cz} dz < \infty.$$

We indicate this set of functions as

$$L^2_\eta := \left\{ v \middle| \int_{\mathbb{R}} e^{\eta z} v^2 dz < \infty \right\}.$$

From equation (2.3.24), we have

$$p_{zz} + cp_z + (1 - 2v_c(z))p = \lambda p. \tag{2.3.25}$$

$$\tilde{q}_{zz} - c\tilde{q}_z + \frac{c^2}{4}\tilde{q} - \frac{c^2}{2}\tilde{q} + c\tilde{q}_z + \left(1 - 2v_c(z)\right)p = \lambda\tilde{q}.$$

$$\tilde{q}_{zz} + \left(1 - 2v_c(z) - \frac{c^2}{4}\right)\tilde{q} = \lambda\tilde{q}.$$

By multiplying both sides by q and the first term is obtained by integration by parts over $\mathbb{R}$, we have:

$$-\int_{\mathbb{R}} \tilde{q}_z^2 dz + \int_{\mathbb{R}} \left(1 - 2v_c(z) - \frac{c^2}{4}\right) \tilde{q}^2 dz = \lambda \int_{\mathbb{R}} \tilde{q}^2 dz. \tag{2.3.26}$$

Now, we would like to show that there are no eigenfunctions for $\lambda > 1$. We re-write $\lambda = 1 + \nu$, thus equation (4.3.31) becomes

$$-\int_{\mathbb{R}} \tilde{q}_z^2 dz - \int_{\mathbb{R}} \left(2v_c(z) + \frac{c^2}{4}\right) \tilde{q}^2 dz = \nu \int_{\mathbb{R}} \tilde{q}^2 dz. \tag{2.3.27}$$

If $c \geq 2$, then $0 < v < 1 \ \forall z \in \mathbb{R}$. Therefore, $2v + \frac{c^2}{4} > 0$. This result implies that $\nu \leq 0$. This means there are no eigenvalues of equation (4.3.26) > 1 when $c \geq 2$.

Remark. In summary, our findings indicate that:
(1) The spectrum located between two parabolas is called the "essential spectrum" and the parabolas themselves are considered as the continuous spectra. It is worth noting that the spectrum in the right half of plane indicates that the travelling waves are unstable for every $c > 0$.
(2) There is no point spectrum of $L(v_c)$ for $\lambda > 1$ when $c \geq 2$.

CHAPTER 3

The existence of solutions of the Fisher-Stefan model

3.1. Introduction of the Fisher-Stefan model

Since the Fisher-KPP equation does not allow the solution to go extinct, the travelling wave cannot replicate the extinction of invasive populations and predict the population in practical situations [**EHMJ+19**]. The Fisher-Stefan model was introduced to overcome this limitation of the Fisher-KPP model [**DL10**], [**BDK12**], [**DG12**], [**DMW14**], [**DMZ14**], [**DL15**], [**GSCR89**]. The Fisher-Stefan model adapts the Fisher-KPP model and includes a moving boundary $x = s(t)$. It can be used to stimulate both biological invasion when the travelling wave speed $c > 0$ and recession when $c < 0$ [**EHMS21**]. This model is characterised by the parameter κ relating the speed of the travelling wave c to the shape of the density front at the moving boundary [**EHMS21**] and has the form

$$u_t = u(1-u) + u_{xx} \quad \text{for} \quad 0 < x < s(t) \quad \text{and} \quad t > 0, \tag{3.1.1}$$

$$u_x(0,t) = 0 \quad \text{at} \quad x = 0, \tag{3.1.2}$$

$$s_t = -\kappa u_x(s(t),t) \quad \text{at} \quad x = s(t), \tag{3.1.3}$$

$$u(s(t),t) = 0, \tag{3.1.4}$$

and

$$s(0) = s_0 \quad \text{and} \quad u(x,0) = u_0(x) \quad 0 < x < s(0), \tag{3.1.5}$$

where $u(x,t)$ denotes the density of the particular population and satisfies the Fisher-KPP equation [**EHMJ+19**].

In this diffusive logistic problem, $x = s(t)$ is the moving boundary that we need to determine. We also have s_0 and κ as constants and the initial function $u_0(x)$ satisfies the following condition [**DL10**]

$$u_0 \in C^2, \quad u_0'(0) = u_0(s_0) = 0, \quad \text{and} \quad u_0 > 0 \quad \text{in} \quad [0, s_0\}. \tag{3.1.6}$$

Since the domain of equation (3.1.1) is bounded to the right by the moving boundary $x = s(t)$, the population density vanishes at $s(t)$. The population density $u(x,t) \geq 0$ depends on the position $0 < x < s(t)$ and time $t > 0$. The parameter $\kappa > 0$ in the Fisher-Stefan model describes the time rate of change of $s(t)$ with the gradient of the density u_x.

Reaction diffusion models with a linear term have been studied by Du and colleagues [**DMW14**], [**DMZ14**], [**DL15**], [**Du20**]. They referred to the extinction or persistence of the travelling waves as a spreading-vanishing dichotomy. In their papers, the initial function $u_0(x)$ represents the population of a new or invasive species at the early stage [**DL10**]. The Fisher-Stefan model assumes that the species invade in the environment from the right end of the initial region, thus $s'(t) = -\kappa u_x(s(t), t)$ [**DL10**]. The carrying capacity is scaled to be $u = 1$ and $u(x, t)$ denotes the density of a certain population. Their motility is represented by a constant diffusion coefficient and the population growth is governed by the logistic growth term. The domain is bounded to the right by a moving boundary $x = s(t)$ at which the population density vanishes [**MEHS22**]. The loss of population at the moving boundary can be described as invasion when $\kappa > 0$ or recession when $\kappa < 0$.

The Fisher-Stefan model holds when $\kappa > 0$. This implies the solutions are dependent on κ and $c \to 0^+$ as $\kappa \to 0^+$ and $c \to 2^-$ as $\kappa \to \infty$ [**DL10**], [**Du20**], [**EHMJ+19**]. This behaviour differs from the Fisher-KPP solutions which evolve to travelling wave profiles when $c > 2$ for $0 < x < \infty$ and the solutions of the trajectories in the phase plane are disregarded when $0 < c < 2$ because the negative population densities grow too large.

We now consider the case at $\kappa < 0$ and the moving boundary $x = s(t)$ goes to the negative x-direction. Indeed, when $-1 < \kappa < 0$ and $s(0)$ is sufficiently large, the solutions of equations (3.1.1) to (3.1.3) move towards receding travelling wave profiles given $s(t) \gg 1$ [**EHMS21**]. This corresponds to the trajectories in the phase-plane at a saddle point. The shape of the travelling wave at $-1 < \kappa < 0$ is qualitatively similar to the travelling wave profiles at $\kappa > 0$ except that the slope becomes steeper as κ decreases [**EHMS21**].

In summary, the two main features distinguishing between the Fisher-Stefan model and the Fisher-KPP model are:
(1) The Fisher-Stefan model includes the moving boundary condition at $x = s(t)$ with $u(s(t), t) = 0$ at $t > 0$.
(2) It allows population to go extinct.

3.2. The existence and uniqueness of solutions of the Fisher-Stefan model

In this section, we look at the boundary condition $x = s(t)$ moving at a constant speed as $t \to \infty$ and let $\tilde{z} = ct - x$. According to Du and Lin [**DL10**], when $0 \le c < 2$, there exists a unique positive solution $u = u_c$ for the following problem

$$\begin{cases} u'' - cu' + u(1-u) = 0 \ \text{ for } \ \tilde{z} > 0, \\ u(0) = 0, \end{cases} \tag{3.2.1}$$

$$u_c(0) = 0 \ \text{ for } \ 0 < \tilde{z} < \infty, \tag{3.2.2}$$

and

$$u_c'(\tilde{z}) > 0 \ \text{ for } \ \tilde{z} \ge 0. \tag{3.2.3}$$

Theorem 3.2.1. *According to lemma 2.2 in Du and Lin* [**DL10**]*, we let* (u, s) *be a solution to equations* (3.1.1) *to* (3.1.3) *defined for* $t \in (0, T_0)$ *for some* $T_0 \in (0, +\infty]$*, then there exist constants* c_1 *and* c_2 *independent of* T_0 *such that:*
$0 < u(t, x) \leq k_1, \quad 0 < s'(t) \leq k_2 \quad for \quad 0 \leq x < s(t)$ *and* $t \in (0, T_0)$.

In our case, we have

$$u'_{c_1}(0) > u'_{c_2}(0) \text{ and } u_{c_1}(z) > u_{c_2}(\tilde{z}) \text{ for } x > 0 \text{ and } c_1 < c_2. \tag{3.2.4}$$

For each $\kappa > 0$, Du and Lin [**DL10**] have shown that there exists a unique $c_0 = c_0(\kappa) > 0$ satisfying

$$\kappa u'_{c_0}(0) = c_0, \tag{3.2.5}$$

where the constant c_0 is the spreading speed.

Next, we would like to analyse equation (3.2.1) to see whether it has positive solutions u^l for all large $l > 0$ and c is positive. According to Du and Lin [**DL10**], there exists $v(\tilde{z})$ such that:

$$v(\tilde{z}) = \begin{cases} u^l(\tilde{z}) \text{ for } 0 \leq \tilde{z} \leq l, \\ \\ 0 \text{ for } \tilde{z} \geq l. \end{cases}$$

Hence, $v(\tilde{z})$ is a lower solution of equation (3.2.1).

The upper solution of equation (3.2.1) for $x \in [0, +\infty)$ is

$$u(\infty) = 1. \tag{3.2.6}$$

Following the lower and upper solution argument from theorem 2.3 in Coster and Habets [**CH01**], there exists at least one solution $u(\tilde{z})$ such that

$$v(\tilde{z}) \leq u(\tilde{z}) \leq 1 \text{ in } [0, +\infty). \tag{3.2.7}$$

Theorem 3.2.2. *According to the spreading-vanishing dichotomy in theorem 3.3 of Du and Lin* [**DL10**] *papers, if we let* $(s(t), t)$*be the solution of the free boundary problem equations* (3.1.1) *to* (3.1.3)*, then the following alternative holds:*
Either
(a) spreading: $s_\infty = +\infty$ *and* $lim_{t\to+\infty} u(x, t) = 1$ *uniformly for* x *in any bounded set of* $(0, +\infty)$*;*
or
(b) vanishing: $s_\infty \leq \frac{\pi}{2}$ *and* $lim_{t\to+\infty} ||u(\cdot, t)||_{C([s(t),0])} = 0$.

From Du and Lin [**DL10**], these two alternatives occur in two cases:
(a) If the initial occupying area $[s_0, 0]$ is beyond a critical size particularly $s_0 \geq \frac{\pi}{2}$, then regardless of the initial population size $u_0(x)$ satisfying equation (3.1.5), spreading always happens. Therefore, $s_\infty > \frac{\pi}{2}$ since $s'(t) > 0$ for $t > 0$.
(b) If $s_0 < \frac{\pi}{2}$, then whether spreading or vanishing occurs is determined by the initial population size u_0 and the coefficient κ in the Stefan-KPP model (assuming other parameters

are fixed).

For such s_0 with each given initial density u_0, spreading or vanishing can happen. This spreading-vanishing dichotomy implies that there exists a non-trivial, non-negative solution of equation (3.2.1) that satisfies

$$0 < u(\tilde{z}) < 1 \text{ for } x \in (0, +\infty),$$

and $u(\tilde{z})$ increases as $\lim_{x\to+\infty} u(\tilde{z}) = 1$.

We re-write equation (3.2.1) as

$$-e^{-c\tilde{z}}u'' + e^{-c\tilde{z}}cu' = e^{-c\tilde{z}}u(1-u).$$

Therefore,

$$-(e^{-c\tilde{z}}u')' = e^{-c\tilde{z}}u(1-u). \tag{3.2.8}$$

As $0 < u(\tilde{z}) < 1$ for $z \in (0, +\infty)$, and $u(1-u) > 0$. Thus,

$$-(e^{-c\tilde{z}}u')' > 0 \text{ for } z \in (0, +\infty).$$

As a result, $e^{-c\tilde{z}}u'(\tilde{z})$ is a decreasing function. Moreover, since $u(\tilde{z})$ is bounded on $(0, +\infty)$, there exists a sequence $\tilde{z}_n \to +\infty$ which satisfies $u'(\tilde{z}_n) \to 0$ as $n \to +\infty$. It follows that $u'(\tilde{z}) > 0$ and $u(\tilde{z})$ is increasing.

In order to prove the uniqueness of the solutions to the Fisher-Stefan equation, we suppose $u_1(z)$ and $u_2(z)$ are positive solutions of equation (3.2.1). We can claim that for any $\epsilon > 0$, there is $w_i(z) = (1+\epsilon)u_i(z)$ to be determined by

$$-(e^{-c\tilde{z}}w_i')' \geq e^{-c\tilde{z}}w_i(1-w_i) \text{ for } i = 1, 2$$

Furthermore, since $\lim_{t\to+\infty} w_i(z) = (1+\epsilon)$, there exists $l_0 > 0$ large satisfiying

$$w_1(l) > u_2(l), \quad w_2(l) > u_1(l) \ \forall l \geq l_0.$$

It follows that

$$(1+\epsilon)u_1(\tilde{z}) \geq u_2(\tilde{z}), \quad (1+\epsilon)u_2(\tilde{z}) \geq u_1(\tilde{z}) \text{ for } 0 < \tilde{z} < l \ \forall l \geq l_0.$$

We thus have $(1+\epsilon)u_1(\tilde{z}) \geq u_2(\tilde{z})$ and $(1+\epsilon)u_2(\tilde{z}) \geq u_1(\tilde{z})$ $\forall \tilde{z} \geq 0$. By letting $\epsilon \to 0$, we can deduce that $u_1 = u_2$. Consequently, we have proved the uniqueness of the solution to equation (3.2.1).

In addition, if $0 \leq c_1 < c_2$ and $u'_{c_i}(\tilde{z}) > 0$, then

$$-u''_{c_1} + c_2 u'_{c_1} > -u''_{c_1} + c_1 u'_{c_1} = u(1-u) \text{ for } \tilde{z} > 0. \tag{3.2.9}$$

Therefore, for any $\epsilon > 0$, $w := (1+\epsilon)u_{c_1}$ satisfies

$$-(e^{-c_2\tilde{z}}w')' \geq e^{-c_2\tilde{z}}w(1-w). \tag{3.2.10}$$

We now consider as $\epsilon \to 0$.

Theorem 3.2.3. *According to the comparison principle in theorem 3.5.3 in Pucci and Serrin* [**PS07**]*, suppose that* $u(\tilde{z})$ *is locally bounded for* $x \in (0, +\infty), c > 0, u_1$ *and* u_2 *are positive solutions of equation* (3.2.1)*, if* $u_{c_1}(\tilde{z})$ *and* $u_{c_2}(\tilde{z})$ *satisfy equation* (3.2.9)*, then* $u_{c_1}(\tilde{z}) \geq u_{c_2}(\tilde{z})$ *for* $\tilde{z} > 0$.

This result indicates that for c_1 and c_2 in equation (3.2.4), we have

$$u'_{c_1}(0) \geq u'_{c_2}(0) \text{ for } c_1 < c_2 < 2.$$

According to Du and Lin [**DL10**], we can evidently conclude that $u_{c_1}(x) > u_{c_2}(x)$ when $x > 0$. Hence, $u'_c(0) > 0$ and $u'_{c_1}(0) > u'_{c_2}(0)$. As a result, $\sigma(c) = c - \kappa u'(0)$ is a strictly increasing function for any fixed $\kappa > 0$. Since $c \to u_c$ is a continuous mapping from $[0, +\infty)$ to $C^1_{loc}[0, +\infty)$, $\sigma(c)$ is also a continuous function. It follows that:

$$\sigma(0) = -\kappa u'_0(0) < 0,$$

and

$$\sigma(+\infty) = +\infty.$$

Consequently, there exists a unique solution $c_0 = c_0(\kappa) > 0$ that satisfies $\sigma(c_0) = 0$.

Since $\lim_{t\to\infty} s(t) = \infty$, if $s'(t)$ approaches a constant c_0 and $v(\tilde{z})$ approaches a positive solution $u(\tilde{z})$ as $t \to \infty$, then $u(\tilde{z})$ must be a positive solution of equation (3.2.1) given $\kappa u'(0) = c$.

Remark. When $0 \leq c < 2$, the solution u_c satisfying equations (3.2.1) to (3.2.3) is given as the stable manifold of the fixed point $(1, 0)$ with $u' > 0$ in the phase portrait of equation (3.2.1).

Remark. The transformation $\tilde{z} = ct - x$ to $z = x - ct$ changes the domain of u_c, but not the appropriately modified limiting behaviour i.e. with $z \to -z$ and so forth. The results in this section also prove the existence of solutions of the Fisher-Stefan model under the usual moving coordinate frame $z = x - ct$.

3.3. The phase portrait analysis of the Fisher-Stefan equation

The density profile analysis of the travelling wave solutions of the Fisher-KPP model can provide insight to the properties and conditions of the Fisher-Stefan model as shown in Figure 8. At $c = 10$ and 2, the solutions are positive and monotonically decreasing. However, at $c = 0.5$, the heteroclinic orbit approaches (0,0) as a spiral, which implies $U(z) < 0$ for various intervals in z [**Mur02a**]. This result indicates that the solutions of the Fisher-KPP model exist for $c < 2$ but they are unstable. Thus, these solutions are often disregarded when $c < 2$ and considered as not exist. This unstable solution has value in describing solution of Fisher-Stefan equation when there are stable solutions to Fisher-Stefan problem.

Previously, in Section 2.3, we have discussed about the travelling wave solutions of the Fisher-KPP model by writing $z = x - ct$ at $c > 0$ as in equation (2.1.5). We now look

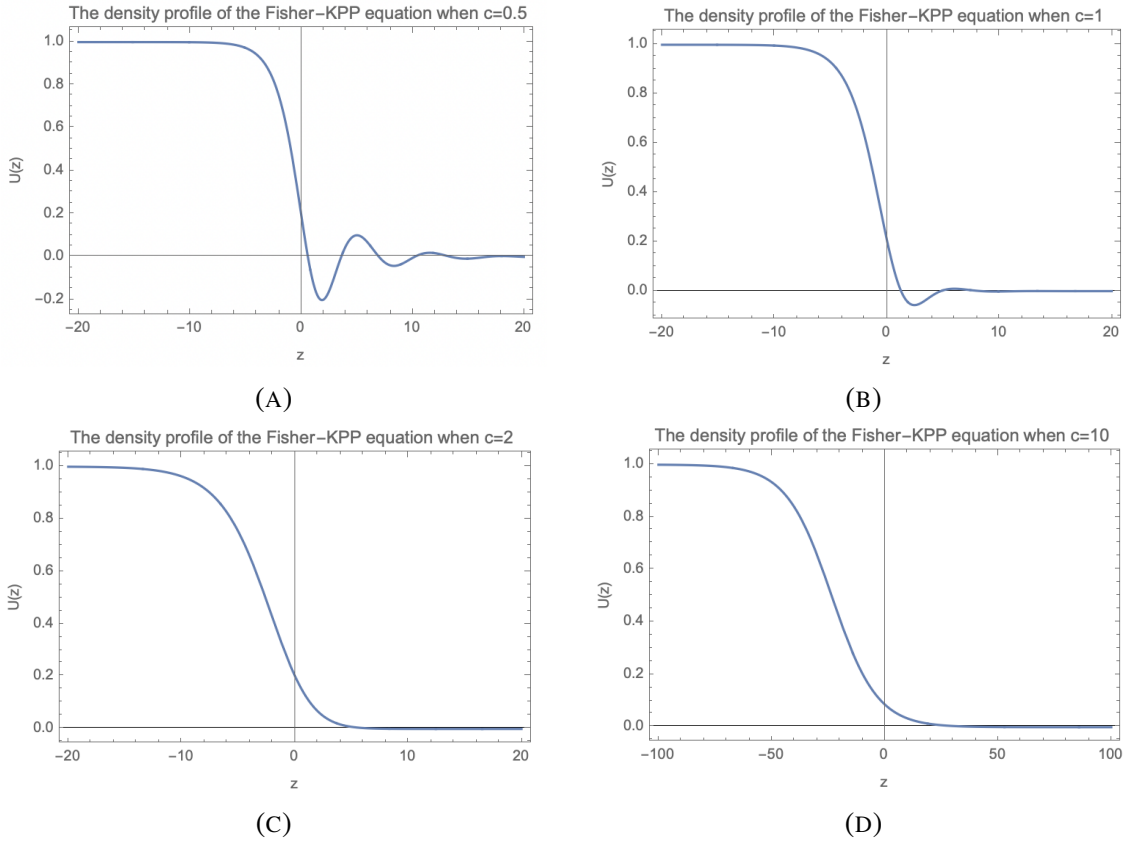

FIGURE 8. Density profiles for the Fisher-KPP equation (1.0.5) when $c = 0.5, 1, 2$ and 10 respectively. We would like to investigate the density profile of the travelling wave solutions of the Fisher-KPP equation as it provides insight to the properties and conditions of the Fisher-Stefan model. At $c = 2$ in Figure (C) and at $c = 10$ in Figure (D), the solutions are positive and monotonically decreasing. However, at $c = 0.5$ and $c = 1$, the heteroclinic orbit approaches (0,0) as a spiral, which implies $U(z) < 0$ for various intervals in z as shown in Figure (A) and (B).

at the phase portrait analysis of the travelling wave solutions to the Fisher-Stefan model.

We would like to find solutions of the form $u(x,t) = U(z)$. This transforms the Fisher-Stefan equation to the second order nonlinear ordinary differential equation

$$\frac{d^2U}{dz^2} + c\frac{dU}{dz} + U(1-U) = 0. \tag{3.3.1}$$

for $-\infty < z < 0$ along with the following boundary conditions [**EHMJ+19**]:

$$U(-\infty) = 1, \quad U(0) = 0, \quad \text{and} \quad c = -\kappa\frac{dU(0)}{dz}. \tag{3.3.2}$$

We will look at $z = 0$ as the moving boundary. Therefore, equation (3.3.1) can be re-written as the first-order system

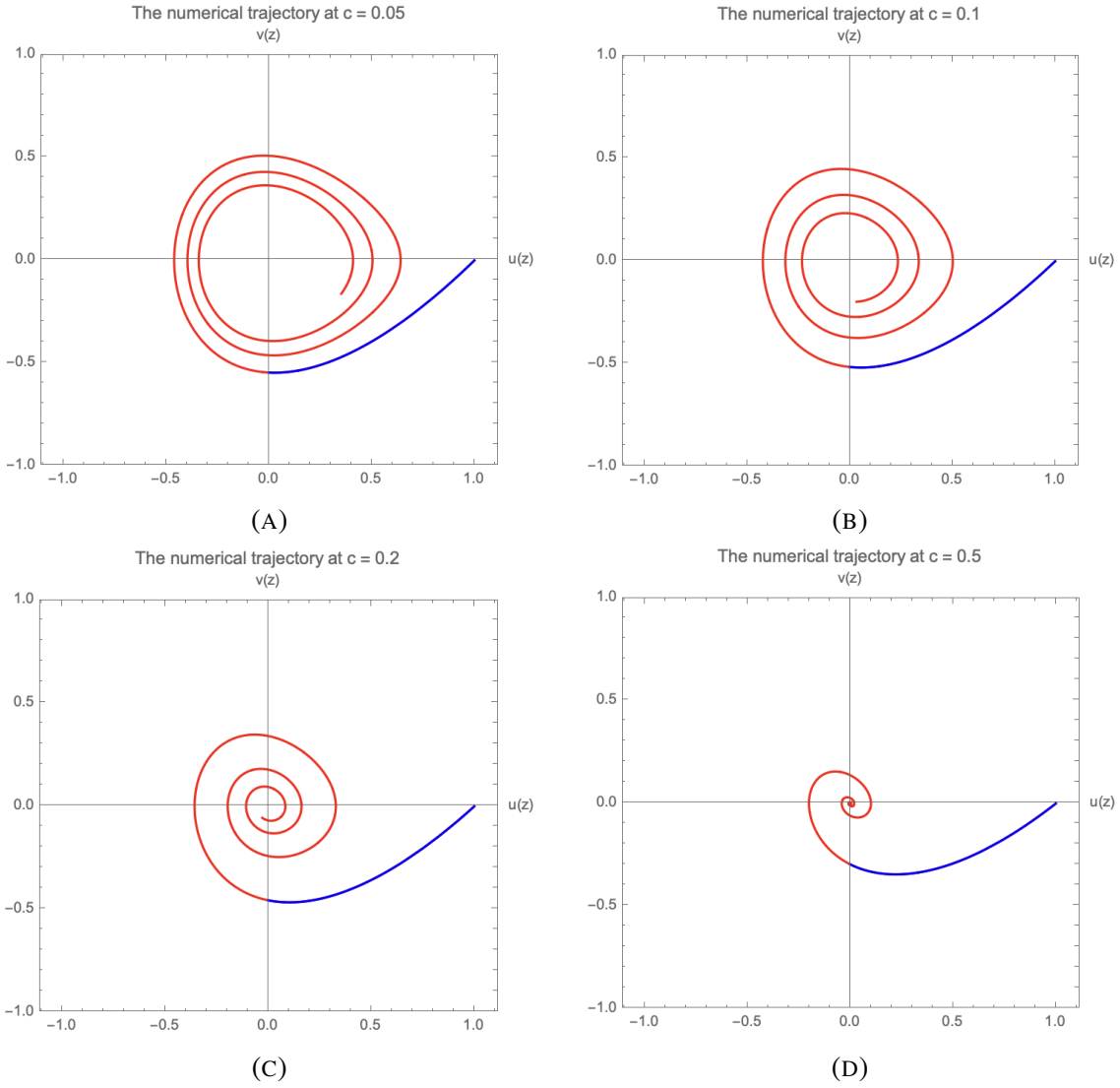

FIGURE 9. The blue curve represents the numerical trajectory of the limiting solutions to the Fisher-Stefan equations (3.1.1) to (3.1.3). The red curve is the solution to the Fisher-KPP equation (1.0.5) when $c = 0.05, 0.1, 0.2$ and 0.5 respectively. We observe that both the Fisher-KPP and the Fisher-Stefan models have the same phase planes (u, v) but with different boundary condition when $0 < c < 2$.

$$\frac{dU}{dz} = V, \tag{3.3.3}$$

and

$$\frac{dV}{dz} = -cV - U(1-U). \tag{3.3.4}$$

with the equilibrium points (0,0) and (1,0). Equation (3.3.3) and equation (3.3.4) are also the dynamical systems of the travelling wave solutions of the Fisher-KPP.

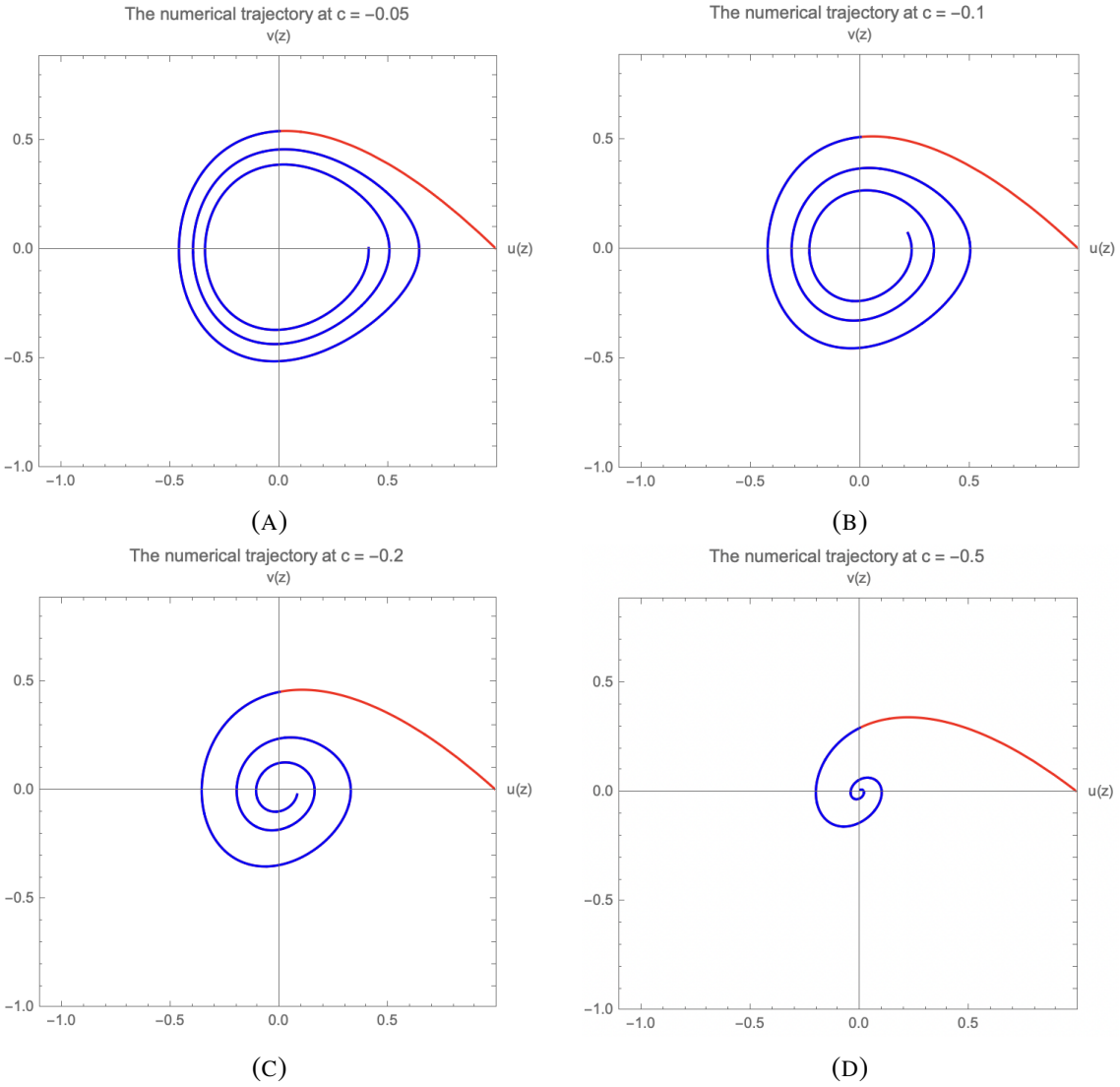

FIGURE 10. The red curve indicates the numerical trajectory of the limiting solutions to the Fisher-Stefan equations (3.1.1) to (3.1.3). The blue curve represents the solution to the Fisher-KPP equation (1.0.5) when $c = -0.05, -0.1, -0.2$ and -0.5 respectively. We conclude that when $-2 < c < 0$, both the Fisher-KPP and the Fisher-Stefan models have the same phase planes (u, v) for asymptotic in time.

Both the Fisher-KPP and the (time asymptotic) Fisher-Stefan equations have the same phase planes (U, V) but with different boundary condition as shown in Figure 9 and Figure 10. Using Mathematica, we observe that for $-2 < c < 0$, the heteroclinic orbit spirals around $(0, 0)$ in Figure 11 while at $c \leq -2$ in Figure 12, it does not. El-Hachem and her colleagues found that since the travelling wave solutions of the Fisher-Stefan model satisfy a different boundary condition, the trajectory must intersect and terminate at the point $\left(0, -\frac{c}{\kappa}\right)$ [**EHMJ+19**]. Hence, the travelling wave solutions of the Fisher-Stefan model exist for all $c < 0$.

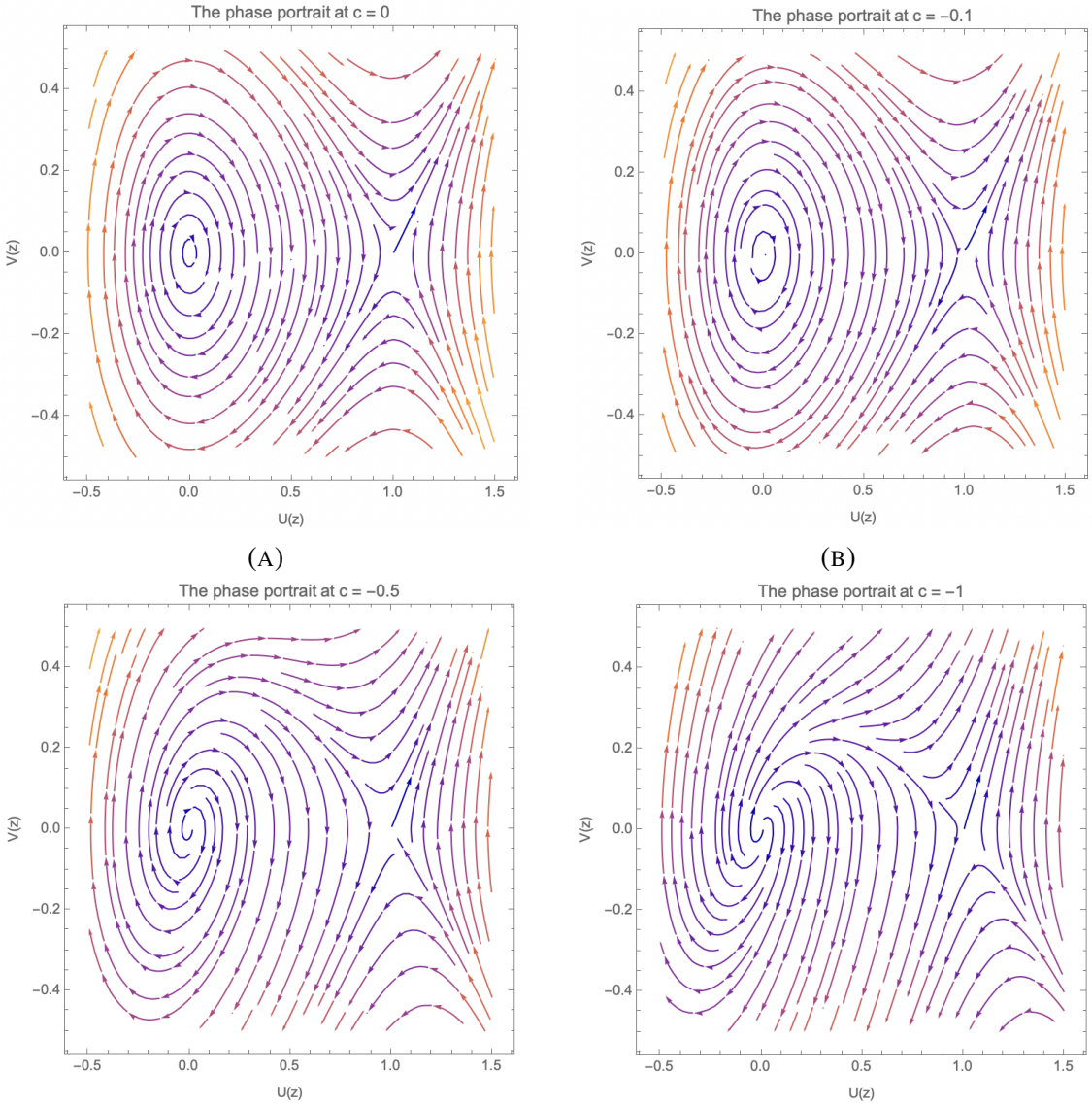

(A) (B)

(C) (D)

FIGURE 11. The phase portrait of the Fisher-Stefan equations (3.3.2) to (3.3.4) at the wave speed $c = 0$, -0.1, -0.5 and -1 respectively. When $-2 < c \leq 0$, the hetericlinic orbit spirals around the origin. We observe that the travelling wave solutions of the Fisher-Stefan model exist in this case.

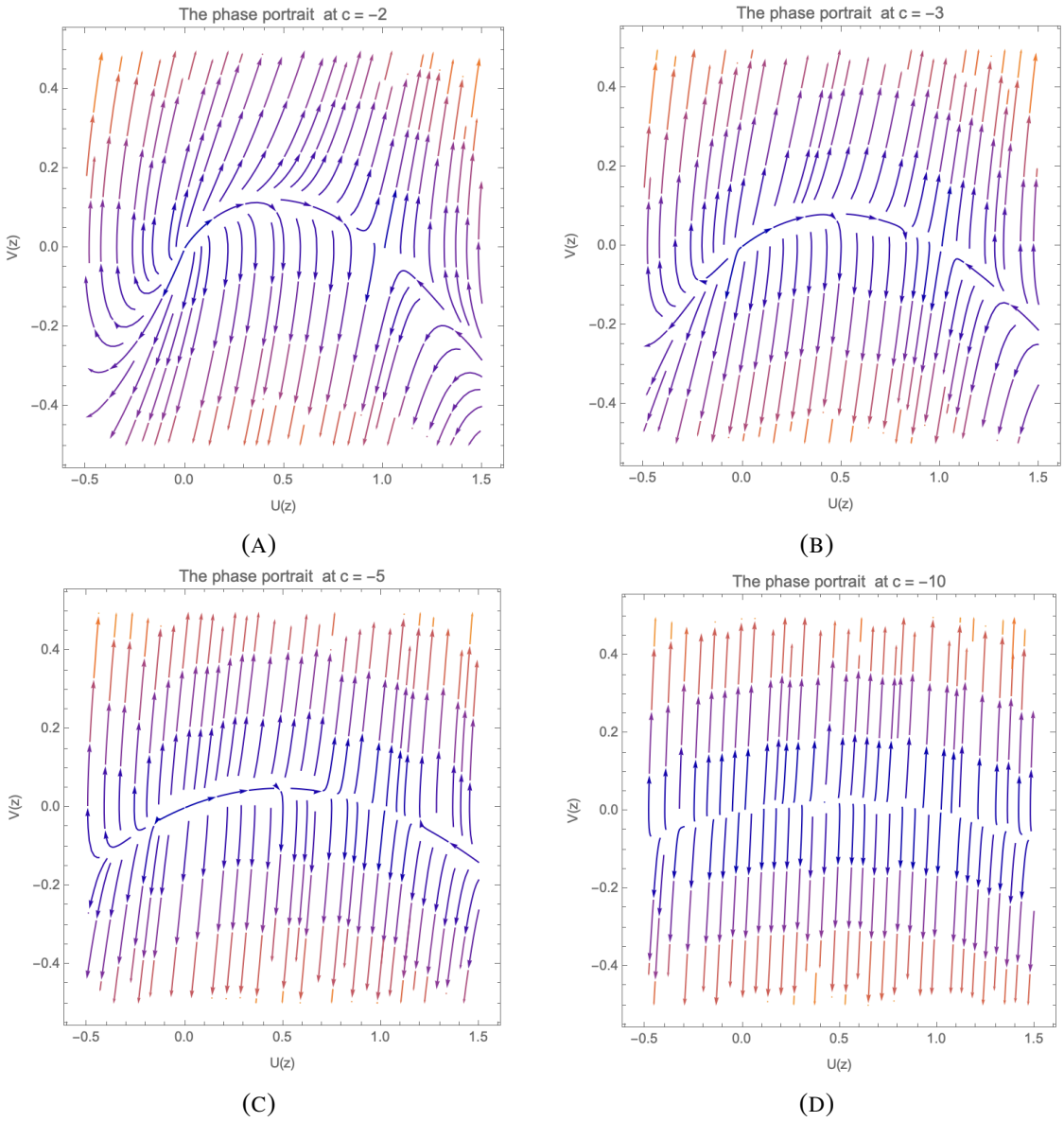

(A) (B)

(C) (D)

FIGURE 12. The phase portrait of the Fisher-Stefan equation (3.3.3) and equation (3.3.4) with the boundary conditions as in equation (3.3.2) at the wave speed $c = -2, -3, -5$ and -10 respectively. When $c \leq -2$, the heteroclinic orbit does not spiral around the origin. However, travelling wave solutions of the Fisher-Stefan model still exist.

CHAPTER 4

The stability of the travelling waves of the Fisher-Stefan model

4.1. Numerical results

We now look at the numerical results of the travelling solutions to the Fisher-Stefan model for $z = x - ct$. According to the phase portrait in Figure 12, we observe that the solutions of equation (3.3.1), which satisfy the boundary condition in equation (3.3.2), exist for all travelling waves of speed $c < 0$. From equation (3.3.3) and equation (3.3.4), as $c \to -\infty$,

$$\frac{dV}{dU} = \frac{-cV + U(1-U)}{V} \sim -c, \tag{4.1.1}$$

which implies the relevant trajectories in the phase plane approach $V = -c\left(U - \frac{1}{\kappa}\right)$. These results can be illustrated by the numerical solutions on the phase portrait in Figure 13.

In Figure 13 and Figure 14, the thick trajectory curve in green of the phase plane represents the travelling wave solutions to this model. Each case always begins at $(U, V) = (1, 0)$ and extends across the fourth quadrant as the trajectories are truncated when c becomes more negative particularly at $c = -0.1, -0.5, -1, -2$ and -5. These results provide us with understanding of the qualitative behaviour of the trajectories and allow us to estimate κ corresponding to specific c and V^0 values in figure 14 where $V^0 := V(U = 0)$. Since the Stefan condition is $c = -\kappa V^0$, this gives us the estimation of κ as the following table:

c	V^0	κ
-0.1	-0.642639	-0.155851
-0.5	-0.928226	-0.538662
-1	-1.32811	-0.752950
-2	-2.21297	-0.903763
-5	-5.09695	-0.980979

Hence, the numerical simulations on Mathematica show that the solutions of the Fisher-KPP equation for $s(0) \gg 1$ evolve toward the travelling profiles with the predicted values of c [**EHMS21**].

4.2. The perturbation solution of the Fisher-Stefan model

In order to describe the shape of the travelling wave solutions to the Fisher-Stefan model for small $c < 2$, we will find perturbation approximations. The perturbation approximation at $c = 0$ corresponding to the asymptotic expansion in the limit as $c \to 0$

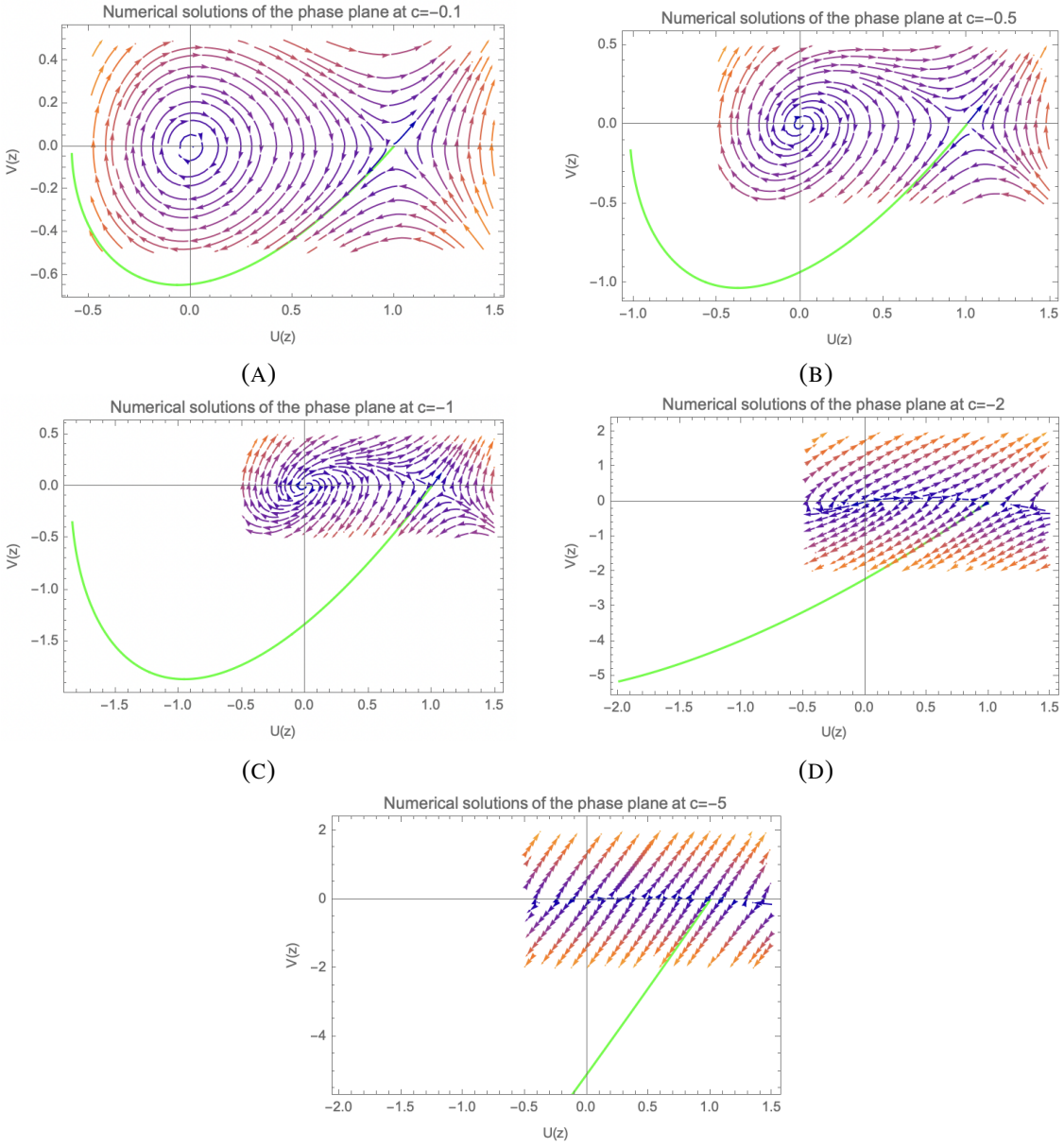

(A) (B) (C) (D) (E)

FIGURE 13. Numerical solutions in the phase plane of the Fisher-Stefan equation (3.3.1) at c = -0.1, -0.5, -1, -2 and -5 respectively. The thick trajectory in green indicates that the solution to this equation satisfies the boundary condition of the Fisher-KPP equation. All cases from (A) to (E) always begin at $(U, V) = (1, 0)$ and extend across the fourth quadrant as the trajectories truncate at the V-axis when c becomes more negative. We also observe that the hetericlinic orbit has unstable spirals around the origin from Figure (A) to (D). These results indicate the travelling wave solutions of the Fisher-Stefan model exist in this case.Thus, the travelling wave solutions of equation (3.3.1) exist when $-\infty < c < 0$. As a result, we can predict the numerical values of κ by solving $c = -\kappa V$ for a particular V value, which allows us to determine the intermediate-time solutions to the moving boundary problem of the Fisher-Stefan model in equation (3.1.1).

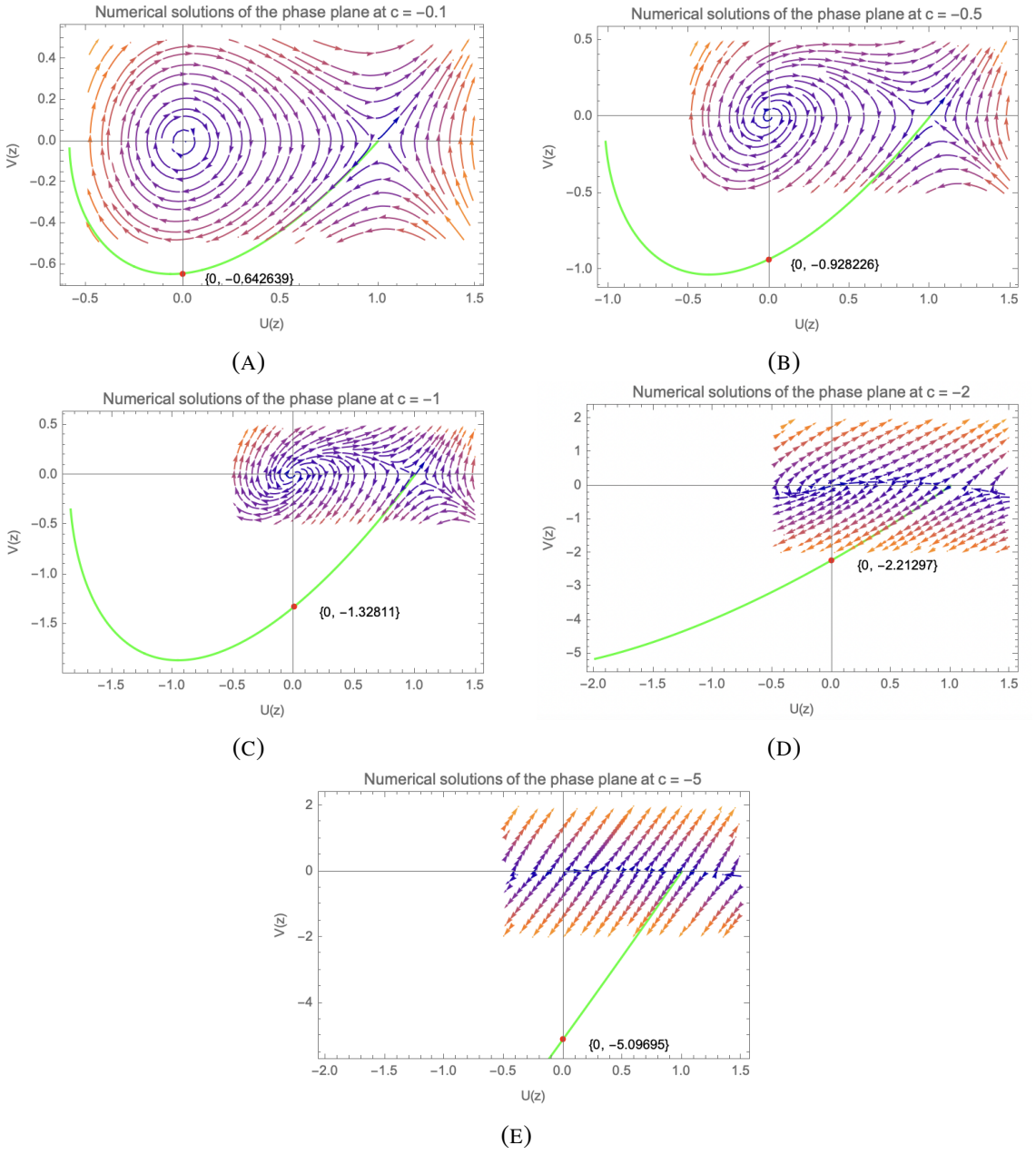

FIGURE 14. Numerical solutions of the phase plane of the Fisher-Stefan equation (3.3.1) and the estimation of V^0 values at $c = -0.1, -0.5, -1, -2$ and -5 respectively. As $c = -\kappa V^0$ in the Fisher-Stefan condition, we can estimate κ values and analyse the qualitative behaviour of the trajectories. At $c = -0.1$, $\kappa \approx -0.155851$, at $c = -0.5$, $\kappa \approx -0.538662$, at $c = -1$, $\kappa \approx -0.752950$, at $c = -2$, $\kappa \approx -0.903763$ and at $c = -5$, $\kappa \approx -0.980979$.

provides useful insight of the invading and receding travelling waves. First, we look at the perturbation solution $|c| \ll 1$ by re-writing $V(U)$ as

$$V(U) = V_0(U) + cV_1(u) + c^2V_2(U) + \mathcal{O}(c^3). \tag{4.2.1}$$

We know that the shape of the stationary travelling wave is

$$\frac{dV}{dU} = \frac{-cV - U(1-U)}{V}. \tag{4.2.2}$$

By substituting equation (4.2.1) into equation (4.2.2), we obtain [**EHMJ+19**]

$$\frac{dV_0}{dU}V_0 + U(1-U) = 0 \text{ at } V_0(1) = 0, \tag{4.2.3}$$

$$\frac{dV_1}{dU}V_0 + \frac{dV_0}{dU}V_1 + V_0 = 0 \text{ at } V_1(1) = 0, \tag{4.2.4}$$

and

$$\frac{dV_2}{dU}V_0 + \frac{dV_0}{dU}V_2 + V_1\left(\frac{dV_1}{dU} + 1\right) = 0 \text{ at } V_2(1) = 0. \tag{4.2.5}$$

The solutions of the differential equation (4.2.3) are

$$\frac{V_0^2}{2} = \frac{U^3}{3} - \frac{U^2}{2} + C. \tag{4.2.6}$$

At $V_0(1) = 0$, we have

$$0 = \frac{1}{3} - \frac{1}{2} + C. \tag{4.2.7}$$

It follows that at $C = \frac{1}{6}$,

$$V_0(U) = -\sqrt{2\left(\frac{U^3}{3} - \frac{U^2}{2} + \frac{1}{6}\right)}, \tag{4.2.8}$$

and

$$V_0(U) = \frac{\sqrt{3(2U+1)}}{3}(U-1). \tag{4.2.9}$$

The solutions of equation (4.2.4) at $V_1(1) = 0$ are

$$\frac{dV_1}{dU}V_0 + \frac{dV_0}{dU}V_1 = -V_0, \tag{4.2.10}$$

$$\frac{d}{dU}\left(V_1V_0\right) = -V_0, \tag{4.2.11}$$

$$V_1V_0 = -\int V_0 dU, \tag{4.2.12}$$

$$\implies V_1 = \frac{-\int V_0 dU}{V_0}. \tag{4.2.13}$$

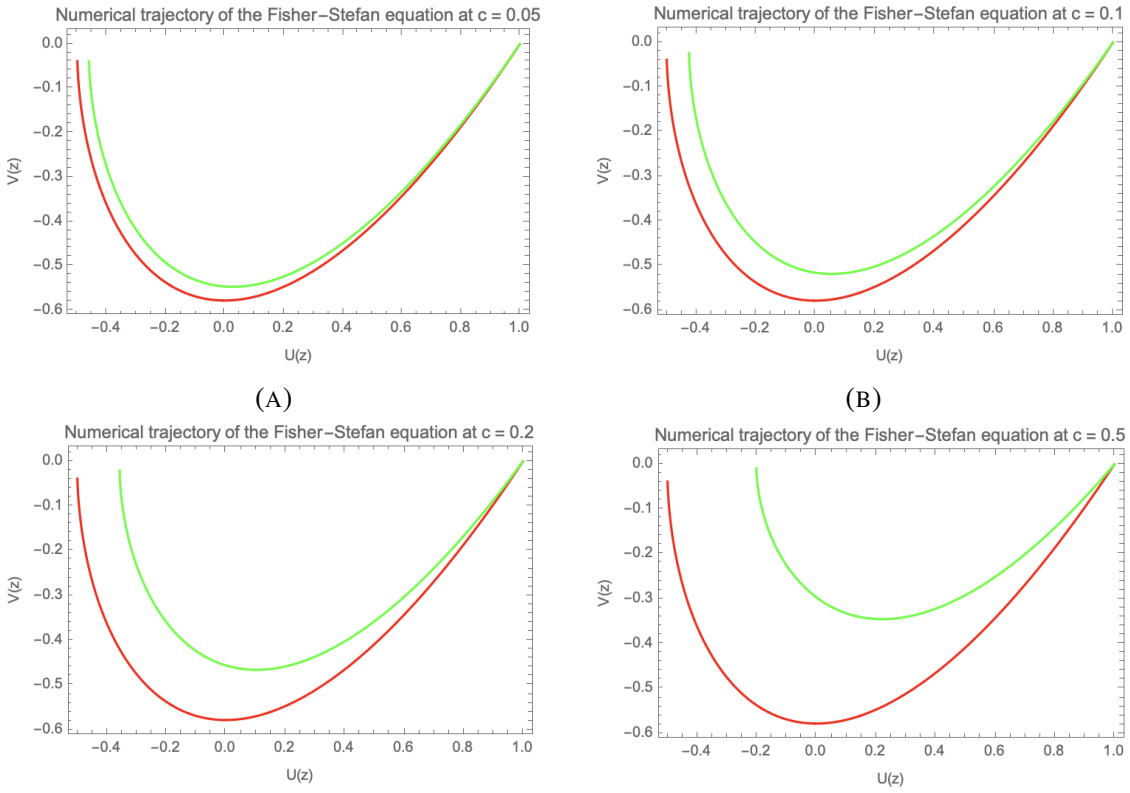

FIGURE 15. Comparison of the approximate trajectories to the Fisher-Stefan equation (3.3.1) between the equilibrium points $(1, 0)$ and $(0, 0)$ in the phase plane at $c = 0.05$, 0.1, 0.2 and 0.5 respectively. The red curves represents the $\mathcal{O}(1)$ perturbation solution of equation (4.2.14) whereas the green curve is the $\mathcal{O}(c)$ perturbation solution of equation (4.2.15).

Since the Fisher-Stefan model satisfies the condition $\kappa = \frac{-c}{V(0)}$ and $V = V(U)$, we can estimate $V(0)$ for $|c| \ll 1$ using the perturbation solution as following [**EHMJ+19**]

$$\mathcal{O}(1) : \kappa = \frac{-c}{V_0(0)}, \tag{4.2.14}$$

$$\mathcal{O}(c) : \kappa = \frac{-c}{V_0(0) + cV_1(0)}, \tag{4.2.15}$$

and

$$\mathcal{O}(c^2) : \kappa = \frac{-c}{V_0(0) + cV_1(0) + c^2V_2(0)}. \tag{4.2.16}$$

To compare the accuracy of $\mathcal{O}(1)$ and $\mathcal{O}(c)$ perturbation solutions for the shape of the $V(U)$ curve, we use Mathematica NDSolve and generate numerical phase planes at $c = 0.05, 0.1, 0.2$ and 0.5 as shown in Figure 9, Figure 15 and all three curves in Figure 16. According to Figure 16, the $\mathcal{O}(1)$ perturbation solution in red curve provides more accurate match to the shape of the numerical solutions in equations (3.1.1) to (3.1.3) at $c = 0.05$. However, as c becomes larger even by $c = 0.5$, the $\mathcal{O}(1)$ solution provides

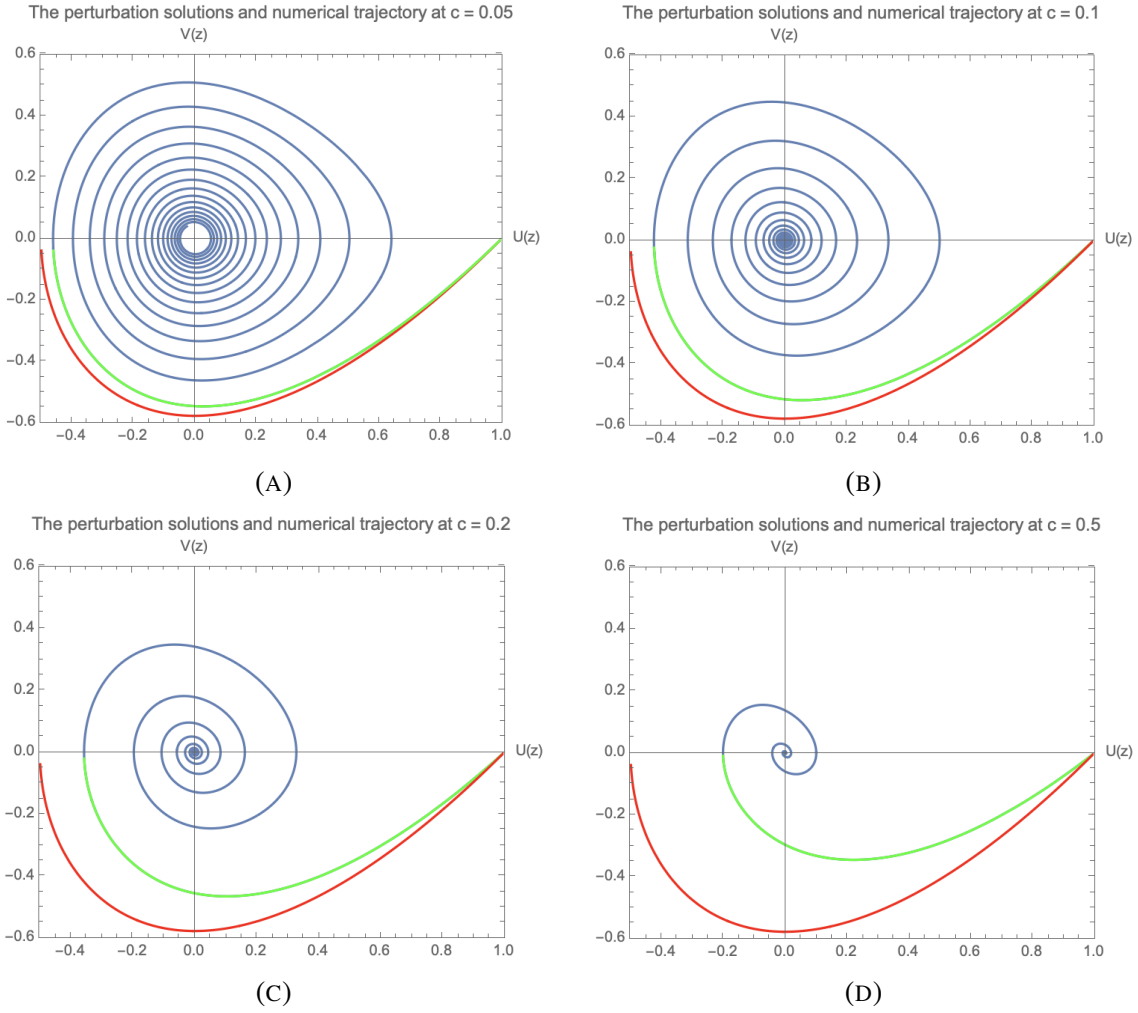

FIGURE 16. The perturbation solutions and numerical trajectories of the Fisher-Stefan equation (3.3.1) between the equilibrium points $(1,0)$ and $(0,0)$ in the phase plane for various c values. The red curve represents the $\mathcal{O}(1)$ perturbation solution of equation (4.2.14). The green curve is the $\mathcal{O}(c)$ perturbation solution of equation (4.2.15) and the blue curve is the numerical trajectories of the Fisher-Stefan model which pass through $\left(0, \frac{-c}{\kappa}\right)$. These plots show that the red curve $\mathcal{O}(1)$ perturbation solution provides more accurate match to the shape of the numerical solutions in equations (3.1.1) to (3.1.3) at $c = 0.05$. However, as c becomes larger especially at $c = 0.5$, it gives poorer approximation. Moreover, the blue and green trajectories resemble each other in the third and fourth quadrants. Thus, the green curve $\mathcal{O}(c)$ perturbation solution can provide a highly-accurate approximation of the shape of the travelling wave solutions of the Fisher-Stefan model at $0 \leq c \leq 0.5$.

poorer approximation. Furthermore, the blue and green trajectories resemble each other in the third and fourth quadrants. This result implies that the $\mathcal{O}(c)$ perturbation solution can provide a highly-accurate approximation of the shape of the travelling wave solutions

of the Fisher-Stefan model when $0 \leq c \leq 0.5$ [**EHMJ+19**].

4.3. Spectral stability of the asymptotic solution to the Fisher-Stefan problem

In this section, we look for solutions of $u(x,t) = j(z,t)$ which solve

$$j_t = j_{zz} + cj_z + j(1-j), \tag{4.3.1}$$

and the set of boundary condition equation (3.3.1) and equation (3.3.2).

We linearise equation (4.3.1) about a fixed $j_c(z)$ and obtain solutions of the form

$$u(z,t) = j_c(z) + \epsilon e^{\lambda t} p(z,t). \tag{4.3.2}$$

By substituting equation (4.3.2) into equation (4.3.1) and $\mathcal{O}(\epsilon)$ terms, we have

$$\lambda p_t = p_{zz} + cp_z + (1 - 2j_c(z))p \tag{4.3.3}$$

$$= \mathcal{L}(j_c(z))p, \tag{4.3.4}$$

with the given conditions

$$p(0) = 0, \tag{4.3.5}$$

and

$$p(-\infty) = 0. \tag{4.3.6}$$

We look at inverting $\mathcal{L}(j_c(z)) - \lambda$ on $L^2_0((-\infty, 0]) =: \mathcal{M}$ such that $\mathcal{L}(j_c(z)) - \lambda$ is not invertible, we need to find $\lambda \in \mathbb{C}$ satisfying the following inhomogeneous equation

$$\mathcal{L}(j_c(z))p - \lambda p = p_{zz} + cp_z + (1 - 2j_c(z))p - \lambda p. \tag{4.3.7}$$

We rewrite equation (4.3.7) as a system

$$\begin{pmatrix} 0 & 1 \\ \lambda - 1 + 2j_c & -c \end{pmatrix} \begin{pmatrix} p \\ q \end{pmatrix} =: A(z;\lambda) \begin{pmatrix} p \\ q \end{pmatrix}, \tag{4.3.8}$$

where $q = p_z$. Finding a Green's function for $\mathcal{L}$ on $\mathcal{M}$ means we need to have decaying solutions in the far-field. As $z \to -\infty$ and $j_c \to 1$, equation (4.3.8) given the boundary condition in equation (3.3.2) becomes

$$\begin{pmatrix} p \\ q \end{pmatrix}_z = \begin{pmatrix} 0 & 1 \\ \lambda + 1 & -c \end{pmatrix} \begin{pmatrix} p \\ q \end{pmatrix} =: A_-(\lambda) \begin{pmatrix} p \\ q \end{pmatrix}, \tag{4.3.9}$$

where

$$\lim_{z \to -\infty} A(z;\lambda) = A_-(\lambda), \tag{4.3.10}$$

and

$$\lim_{z\to-\infty} j_c(z) = 1. \tag{4.3.11}$$

Next we will find decaying solutions and look at the continuous spectrum of the travelling waves to the Fisher-Stefan model.

4.3.1. The asymptotic operator and continuous spectrum of the Fisher-Stefan model.

We now consider solutions to the constant coefficient equation

$$\begin{pmatrix} p \\ q \end{pmatrix}_z = A_-(\lambda) \begin{pmatrix} p \\ q \end{pmatrix} \quad \text{for } z < 0, \tag{4.3.12}$$

where the asymptotic operator is defined as

$$\mathcal{L}_\infty := \partial_{zz} + c\partial_z - 1. \tag{4.3.13}$$

We look for the spectrum of $\mathcal{L}_\infty$. As we have discussed in Chapter 2 and based on Weyl's essential spectrum theorem in Kapitula and Promislow, any spectrum of $\mathcal{L}_\infty$ will be the same as the spectrum of $\mathcal{L}$ up to the point spectrum [**KP13**].

The general solution to equation (4.3.9) is

$$\begin{pmatrix} p \\ q \end{pmatrix}_z = c_1 e^{\mu_-(\lambda)z} \begin{pmatrix} 1 \\ \mu_-(\lambda) \end{pmatrix} + c_2 e^{\mu_+(\lambda)z} \begin{pmatrix} 1 \\ \mu_+(\lambda) \end{pmatrix}, \tag{4.3.14}$$

where $\mu_\pm(\lambda)$ are the eigenvalues of the matrix $A_-(\lambda)$.

The eigenvalues in equation (4.3.14) are the roots of its characteristic equation

$$\det(A_-(\lambda) - \mu) = \mu^2 + c\mu - (\lambda + 1) = 0. \tag{4.3.15}$$

We can express equation (4.3.15) in terms of λ as following

$$\mu_\pm^{-\infty}(\lambda) = \frac{1}{2}\left(-c \pm \sqrt{c^2 + 4(\lambda + 1)}\right). \tag{4.3.16}$$

We would like to invert the operator $\mathcal{L}_\infty$ in equation (4.3.13) by finding decaying solutions qualitatively depending on λ. We will look at the values of λ so that the real parts of $\mu_\pm$ vanish for $k \in \mathbb{R}$. We begin with a real $\lambda \gg 1$ at $\mu_\pm(\lambda)$ and observe that $\mu_-(\lambda) > 0$ when $\mu_+(\lambda) < 0$. Hence, we have the solution corresponding to $\mu_+(\lambda)$ decaying as $z \to -\infty$.

At $z = 0$, the solution is

$$\eta_u(0) := c_2 \begin{pmatrix} 1 \\ \mu_-(\lambda) \end{pmatrix}. \tag{4.3.17}$$

In order to invert $\mathcal{L}$, we solve $(\mathcal{L}_\infty - \lambda)p = \delta(x)$ and write the Green's function as

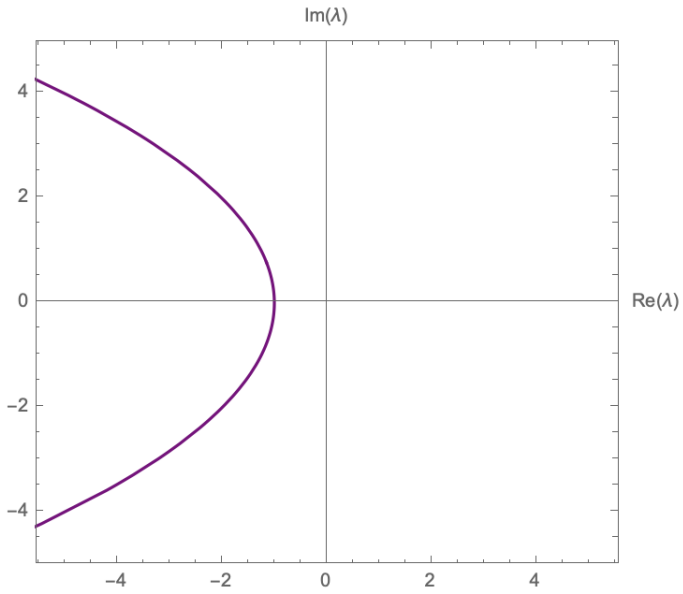

FIGURE 17. This is the continuous spectrum of the travelling waves of the Fisher-Stefan model. It is shown as the purple curve, which represents the set where $A_-(\lambda)$ has a purely imaginary eigenvalue and $k \in \mathbb{R}$ is the imaginary part of the eigenvalue $A_-(\lambda)$ in equation (4.3.19) at $c = 2$. This continuous spectrum is strictly in the left half plane. For λ to the right of this curve, the signature of $A_-(\lambda)$ is $(-1, 1)$. For λ to the left, the signature of $A_-(\lambda)$ is $(-1, -1)$.

$$G(z, \eta; \lambda) = c_2 e^{\mu_-(\lambda)(z-\eta)} \begin{pmatrix} 1 \\ \mu_-(\lambda) \end{pmatrix} \quad \text{for } z \leq \eta. \tag{4.3.18}$$

Now we look for λ so that the real parts of $\mu_\pm$ vanish by letting $\det(A_\pm - ik) = 0$ and re-arrange for λ to obtain

$$\lambda_- = -k^2 - 1 + ick. \tag{4.3.19}$$

Equation (4.3.19) is a parametrised curve of $\lambda \in \mathbb{C}$, opening leftwards in the complex plane. This single parabola represents the continuous spectrum of the travelling waves to the Fisher-Stefan equation as shown in Figure 17. The parametric variable k is the imaginary part of the eigenvalue $A_-(\lambda)$. In this case, the spectrum is always on the left half plane. For λ to the right of this curve, the signature of $A_-(\lambda)$ is $(-1, 1)$ (one negative eigenvalue and one positive eigenvalue). For λ to the left of this curve, the signature of $A_-(\lambda)$ is $(-1, -1)$. The fact that $A_-(\lambda)$ has two negative eigenvalues, this implies the asymptotic operator $\mathcal{L}_\infty$ is invertible according to lemma 3.1.10 in Kapitula and Promislow [**KP13**].

4.3.2. Point spectrum of the Fisher-Stefan asymptotic solution.

In this part, we will look for a $\lambda \in \Omega$ to the right of the continuous spectrum so that

$$\mathcal{L}(j_c)p = \lambda p, \tag{4.3.20}$$

and

$$\lim_{x\to-\infty} x = 0. \tag{4.3.21}$$

We begin with solutions to equation (4.3.20) and let

$$q = e^{\frac{c}{2}z}p. \tag{4.3.22}$$

In order for $p \in L^2\mathbb{R}$,

$$\int_{\mathbb{R}} e^{-cz}q^2 dz < \infty, \tag{4.3.23}$$

and $q \in L^2$, we must have

$$\int p^2 e^{cz} dz < \infty. \tag{4.3.24}$$

Let us denote this set of functions as

$$L^2_\iota := \left\{ j \middle| \int_{\mathbb{R}} e^{\iota z} j^2 dz < \infty \right\}. \tag{4.3.25}$$

We can also write equation (4.3.20) as

$$p_{zz} + cp_z + (1 - 2v_c(z))p = \lambda p. \tag{4.3.26}$$

Therefore,

$$q_{zz} + \left(1 - 2v_c(z) - \frac{c^2}{4}\right) q = \lambda q. \tag{4.3.27}$$

By multiplying both sides by q and integrating over $(-\infty, 0]$, since

$$\int_{-\infty}^{0} q_{zz} q dz = q(0)q_z(0) - \int_{-\infty}^{0} q_z^2 dz = -\int_{-\infty}^{0} q_z^2 dz, \tag{4.3.28}$$

we obtain

$$-\int_{-\infty}^{0} q_z^2 dz + \int_{-\infty}^{0} \left(1 - 2v - \frac{c^2}{4}\right) q^2 dz = \lambda \int_{-\infty}^{0} q^2 dz. \tag{4.3.29}$$

Previously in section 4.3.1, we have shown that the continuous spectrum of $\mathcal{L}(j_c)$ in the space $\mathcal{M}$ of the Fisher-Stefan model is strictly in the left half plane as in Figure 17. Suppose we had an eigenvalue λ to $\mathcal{L}(j_c)$ for some λ to the right of this curve, then there would exist a solution p satisfying $\mathcal{L}p = \lambda p$ for $p \in L^2(\mathbb{R})$. Since p decays as $z \to -\infty$, we must have

$$p \sim e^{z\left(\frac{-c}{2}+\sqrt{\lambda+1+\frac{c^2}{4}}\right)}. \tag{4.3.30}$$

We would like to show that there are no eigenfunctions with $\lambda > 1$. By rewriting $\lambda = 1+\gamma$, equation (4.3.28) becomes

$$-\int_{-\infty}^{0} q_z^2 dz - \int_{-\infty}^{0} \left(2v + \frac{c^2}{4}\right) q^2 dz = \gamma \int_{-\infty}^{0} q^2 dz. \tag{4.3.31}$$

If $c \geq 0$, then $0 < v < 1$ for $z \in (-\infty, 0]$. This result implies that there are no such $\lambda \in \sigma$ such that $\lambda > 1$ $\forall c \geq 0$. We can conclude that there is no point spectrum of $\mathcal{L}(j_c)$ for $\lambda > 1$ for all real $c \geq 0$ in the Fisher-Stefan equation.

Remark. In a nutshell, our findings indicate that:
(1) The continuous spectrum of the travelling waves to the Fisher-Stefan model represents the set $A\_(\lambda)$, which has a purely imaginary eigenvalue and $k \in \mathbb{R}$ is the imaginary part of the eigenvalue $A\_(\lambda)$ in equation (4.3.19) at $c > 0$. This continuous spectrum is strictly in the left half plane and the asymptotic operator $\mathcal{L}_\infty$ is invertible.
(2) There is no point spectrum of $\mathcal{L}(v_c)$ for $\lambda > 1$ when $c \geq 0$.

CHAPTER 5

Conclusion and future work

In this thesis, we focus on analysing the existence of the solutions, the phase plane (u, v) and the stability of the standing waves and (asymptotic) travelling waves in the Fisher-KPP and Fisher-Stefan models. We look at constant solutions at two fixed points $u = 0$ and $u = 1$, the vector field near $(u, v) = (0, 0)$ and the behaviour of the dynamical system near these two equilibrium points. We have found that $(0, 0)$ is a stable node for $c \geq 2$ and stable spiral for $0 < c < 2$ whereas $(1, 0)$ is a saddle point for all $c \in \mathbb{R}$. By discussing about the asymptotic operator, the continuous spectrum and the point spectrum, we establish the similarities and differences between the two models. Our findings indicate that in the Fisher-KPP case, the essential spectrum is located between two parabolas and the parabolas themselves are called the continuous spectra. The spectrum in the right half plane is unstable for every c value. There is no point spectrum of $\mathcal{L}(v_c)$ for $\lambda > 1$ and $c \geq 0$. In the Fisher-Stefan case, the continuous spectrum is strictly in the left half plane. Thus, the asymptotic operator $\mathcal{L}_\infty$ is invertible. There is also no point spectrum $\mathcal{L}(j_c)$ for $\lambda > 1$ and $0 < c < 2$.

Moreover, the analysis contained in this thesis considers the spectral stability of waves in the Fisher-KPP and the Fisher-Stefan problems. The Fisher-KPP equation is a well-known dynamical system and the stability of its waves has been studied by many researchers [**Can73**], [**DL10**], [**EK**], [**EHMJ+19**], [**GSCR89**], [**Mur02b**]. In the study by El-Hachem and her colleagues, they directly compared the travelling waves of these two models [**EHMJ+19**]. A feature of the Fisher-KPP equation is that the waves of speed $c < 2$ are unstable [**EHMJ+19**] due to their continuous spectrum in the right half plane. This is a weakness of the Fisher-KPP equation according to Griffith and his colleagues because small translocated populations do not always invade and can possibly go extinct [**GSCR89**]. However, the Fisher-Stefan equation supports travelling wave solutions for $c < 2$ and can predict the extinction of particular initial populations, which is referred as the spreading-vanishing dichotomy [**EHMJ+19**]. In this thesis, our results demonstrate that in the Fisher-KPP model, when $c < 2$, there are no stable waves whereas in the Fisher-Stefan model, there exist waves that are stable in time for $0 < c \leq 2$. Du and Lin also researched about the spreading-vanishing dichotomy and the asymptotic behaviour of the solution to the Fisher-Stefan equation [**DL10**]. They proved that this was the time asymptotic solution [**DL10**], however they did not address the spectral stability of the problem. This thesis provides further understanding of the Fisher-Stefan model and spectral justification for stability of these waves. Since these waves are potentially spectrally stable, it is also possible to analyse them in terms of other types of stability such as non-linear, asymptotic or linear stability, a topic for future study.

The numerical simulation of the Fisher-Stefan model allows us to construct approximate solutions and determine the relationship between κ and c. By solving $c = -\kappa V^0$ for

a particular V^0 value, we can predict the numerical values of κ. We also compare the numerical trajectories of the Fisher-Stefan model between the equilibrium points $(0, 0)$ and $(1, 0)$ in the phase plane for various wave speed c. Our numerical results show that $\mathcal{O}(1)$ perturbation solution provides a poor approximation as c becomes larger. However, $\mathcal{O}(c)$ perturbation solution gives a more accurate estimation between the shape of the travelling waves solutions and c values when $c < 0.5$.

For future work, we would like to show full spectral stability, i.e. that there are no eigenvalues to the Fisher-Stefan problem with $\lambda > 0$ for $c > 0$. The study by Harley and her colleagues demonstrated a geometric technique to show spectral stability of the Fisher-KPP equation and by doing this, they vertified the absence of eigenvalues in the right half plane [**HvHM+15**]. One avenue is to use a similar method developed by their research to identify whether it is feasible to apply in the case of the half line.

We can also look at other classes of models using different source terms to analyse the stability of travelling wave solutions including a nonlinear Allee effect. This method was also examined earlier by Du and Guo [**DG12**]. They described the Allee effect as populations may shrink at very low densities [**DG12**]. This effect can be incorporated in the Fisher-KPP model by replacing the logistic reaction term by a bistable reaction term. The strong Allee effect is when a species begins with a small initial population and then eventually dies out [**DPS19**]. Such a model has a bistable reaction term. Further, in this paper, Du, Peng and Sun introduced a protection zone, to save endangered species, and governed by the Fisher-KPP nonlinearity. Their work focused on investigating the dynamics of a reaction-diffusion model, the strong Allee effect and the protection zone to prove a so-called vanishing-transition-spreading trichotomy [**DPS19**]. Another study by Manoranjan and co-authors focused on the Fisher-KPP population model and a time-dependent Allee threshold [**M+20**]. They employed the generalised Riccati equation mapping approach to find exact travelling wave solutions, and recovered the travelling wave solution of the degenerate Fitzhugh-Nagumo equation when the time-dependent Allee threshold decayed to a constant value [**M+20**]. Exploration of the effects of an Allee nonlinearity seems to be a wide potential area for future study.

References

[Ada17] M. Adams. Catching travelling waves with the freezing method, 2017. Honours Thesis. [Page 15.]

[AW75] Donald G Aronson and Hans F Weinberger. Nonlinear diffusion in population genetics, combustion, and nerve pulse propagation. In *Partial differential equations and related topics*, pages 5–49. Springer, 1975. [Page 7.]

[BDK12] Gary Bunting, Yihong Du, and Krzysztof Krakowski. Spreading speed revisited: analysis of a free boundary model. *Networks & Heterogeneous Media*, 7(4):583, 2012. [Page 34.]

[Can73] José Canosa. On a nonlinear diffusion equation describing population growth. *IBM Journal of Research and Development*, 17(4):307–313, 1973. [Pages 7, 55.]

[CH01] C De Coster and P Habets. An overview of the method of lower and upper solutions for odes. *Nonlinear analysis and its applications to differential equations*, pages 3–22, 2001. [Page 36.]

[DG12] Yihong Du and Zongming Guo. The stefan problem for the fisher–kpp equation. *Journal of Differential Equations*, 253(3):996–1035, 2012. [Pages 34, 56.]

[DL10] Yihong Du and Zhigui Lin. Spreading-vanishing dichotomy in the diffusive logistic model with a free boundary. *SIAM Journal on Mathematical Analysis*, 42(1):377–405, 2010. [Pages 10, 34, 35, 36, 38, 55.]

[DL15] Yihong Du and Bendong Lou. Spreading and vanishing in nonlinear diffusion problems with free boundaries. *Journal of the European Mathematical Society*, 17(10):2673–2724, 2015. [Pages 34, 35.]

[DMW14] Yihong Du, Hiroshi Matano, and Kelei Wang. Regularity and asymptotic behavior of nonlinear stefan problems. *Archive for Rational Mechanics and Analysis*, 212(3):957–1010, 2014. [Pages 34, 35.]

[DMZ14] Yihong Du, Hiroshi Matsuzawa, and Maolin Zhou. Sharp estimate of the spreading speed determined by nonlinear free boundary problems. *SIAM Journal on Mathematical Analysis*, 46(1):375–396, 2014. [Pages 34, 35.]

[DPS19] Kai Du, Rui Peng, and Ningkui Sun. The role of protection zone on species spreading governed by a reaction–diffusion model with strong allee effect. *Journal of Differential Equations*, 266(11):7327–7356, 2019. [Page 56.]

[Du20] Yihong Du. Propagation, diffusion and free boundaries. *SN Partial Differential Equations and Applications*, 1(5):1–25, 2020. [Page 35.]

[EHMJ+19] Maud El-Hachem, Scott W McCue, Wang Jin, Yihong Du, and Matthew J Simpson. Revisiting the fisher–kolmogorov–petrovsky–piskunov equation to interpret the spreading–extinction dichotomy. *Proceedings of the Royal Society A*, 475(2229):20190378, 2019. [Pages 11, 34, 35, 39, 41, 47, 48, 50, 55.]

[EHMS21] Maud El-Hachem, Scott W McCue, and Matthew J Simpson. Invading and receding sharp-fronted travelling waves. *Bulletin of Mathematical Biology*, 83(4):1–25, 2021. [Pages 34, 35, 44.]

[EK] L Edelstein-Keshet. Mathematical models in biology, siam, philadelphia,(2005). [Page 55.]

[Fis37] Ronald Aylmer Fisher. The wave of advance of advantageous genes. *Annals of eugenics*, 7(4):355–369, 1937. [Pages 7, 8.]

[Gri02] David H Griffel. *Applied functional analysis*. Courier Corporation, 2002. [Page 23.]

[Gro59] David M. Grobman. Homeomorphism of systems of differential equations,. *Doklady Akad. Nauk SSSR*, 128:880–881, 1959. [Page 16.]

[Gro62] David M. Grobman. Topological classification of neighborhoods of a singularity in n-space. *Mat. Sbornik*, 56(98):77–94, 1962. [Page 16.]

[GSCR89] Brad Griffith, J Michael Scott, James W Carpenter, and Christine Reed. Translocation as a species conservation tool: status and strategy. *Science*, 245(4917):477–480, 1989. [Pages 34, 55.]

[Har60] Philip Hartman. A lemma in the theory of structural stability of differential equations,. *Proceedings of the American Mathematical Society*, 11:610–620, 1960. [Page 16.]

[Har63] Philip Hartman. On the local linearization of differential equations. *Proceedings of the American Mathematical Society*, 14:568–573, 1963. [Page 16.]

[HvHM+15] Kristen Harley, Petrus van Heijster, Robert Marangell, GJ Pettet, and Martin Wechselberger. Numerical computation of an evans function for travelling waves. *Mathematical biosciences*, 266:36–51, 2015. [Page 56.]

[KP13] Todd Kapitula and Keith Promislow. *Spectral and dynamical stability of nonlinear waves*, volume 457. Springer, 2013. [Pages 22, 26, 28, 51, 52.]

[LMLNC03] Simon A Levin, * Helene C Muller-Landau, * Ran Nathan, and * Jérôme Chave. The ecology and evolution of seed dispersal: a theoretical perspective. *Annual Review of Ecology, Evolution, and Systematics*, 34(1):575–604, 2003. [Page 7.]

[M+20] Valipuram Manoranjan et al. Analysis of the fisher-kpp equation with a time-dependent allee effect. *IOP SciNotes*, 1(2):025003, 2020. [Page 56.]

[MEHS22] Scott W McCue, Maud El-Hachem, and Matthew J Simpson. Traveling waves, blow-up, and extinction in the fisher–stefan model. *Studies in Applied Mathematics*, 148(2):964–986, 2022. [Page 35.]

[Mei07] James D Meiss. *Differential dynamical systems*. SIAM, 2007. [Page 19.]

[Mur02a] James D Murray. Mathematical biology: I. an introduction. interdisciplinary applied mathematics. *Mathematical Biology, Springer*, 17, 2002. [Page 38.]

[Mur02b] JD Murray. Models for interacting populations. *Mathematical biology: I. An introduction*, pages 79–118, 2002. [Page 55.]

[PS07] Patrizia Pucci and James Serrin. Maximum principles for elliptic partial differential equations. *Handbook of differential equations–stationary partial differential equations*, 4:355–483, 2007. [Page 38.]

[She98] Jonathan A Sherratt. On the transition from initial data to travelling waves in the fisher-kpp equation. *Dynamics and Stability of Systems*, 13(2):167–174, 1998. [Page 7.]

[Ske51] John Gordon Skellam. Random dispersal in theoretical populations. *Biometrika*, 38(1/2):196–218, 1951. [Page 7.]

[SKT95] Nanako Shigesada, Kohkichi Kawasaki, and Yasuhiko Takeda. Modeling stratified diffusion in biological invasions. *The American Naturalist*, 146(2):229–251, 1995. [Page 7.]

[ST84] Brian D Sleeman and E Tuma. On exact solutions of a class of reaction-diffusion equations. *IMA journal of applied mathematics*, 33(2):153–168, 1984. [Page 7.]